

Building Mangrove Capital

Assessing the Benefit-Cost Ratio for Mangrove
Restoration Across the Wider Caribbean



BUILDERS
INITIATIVE

Building Mangrove Capital

Assessing the Benefit- Cost Ratio for Mangrove Restoration Across the Wider Caribbean

Pelayo Menéndez¹
Chris Lowrie¹
Michael W. Beck¹

1. Institute of Marine Sciences, 115 McAllister
Way, University of California, Santa Cruz, CA
95060, USA.

Cover and back cover image: Sunset over
a saltwater tidal creek and mangrove
forest on the island of Eleuthera, The
Bahamas. © Erik Kruthoff.

Graphic Design: .Puntoaparte Editores.

Suggested Citation: Menéndez, P., Lowrie, C.,
and Beck, M. W. (2022). "Building Mangrove
Capital: Assessing the Benefit Cost Ratio
for Mangrove Restoration Across the Wider
Caribbean." The Nature Conservancy,
Arlington, VA.

We gratefully acknowledge the funding of AXA XL and
Builders Initiative Foundation.

This report is the second of three reports to be released by
TNC in collaboration with our partners at AXA XL, CIN-
VESTAV, and the University of California, Santa Cruz. The
reports are part of a project aimed at assessing the feasibil-
ity for a mangrove insurance product in the Gulf of Mexico
and Caribbean. In the first report, we document the types
of mangrove damages that may result from hurricanes, the
appropriate restoration techniques to adequately restore
damaged mangroves, and the costs of these restoration
efforts. In this second report, we document the protective
value of mangrove forests in the study region. Finally, in
the final report, we aggregate information from the first
two reports and identify specific areas where a mangrove
insurance product would be most cost-effective. We also
summarize the efforts of our market analysis in Mexico,
Florida, and The Bahamas and identify specific locations
where a mangrove insurance product could be piloted. Trop-
ical storms and hurricanes can cause significant damages
to mangroves and restoration costs can be high. Financing
these restoration activities, through innovative solutions like
an insurance product, will be critical to ensuring that the
protective benefits of mangroves are sustained in the future.

The work for this report was conducted from March 2021
through September 2022. The findings do not take into
account any impacts or changes that may have resulted
from the landfall of Hurricane Ian in late September 2022.



Executive Summary

Coastal ecosystems such as reefs and mangroves act as natural barriers to waves and storm surge, reducing flood damages to people and property. These ecosystem benefits are critical across the Caribbean, where there have been substantial increases in storm risk and extensive habitat loss over the past 30 years.

We assessed flood risk to coastal communities across the Caribbean and identified the long-term benefits from mangroves and the return on investment (ROI) of mangrove restoration for flood risk reduction. We also developed a mangrove fragility curve that identifies potential losses of mangrove habitats based on extreme wind speeds. Using global asset data (2020 USD), we find that Mexico (6.26 billion), The Bahamas (2.29 billion), and Florida (13.10 billion) had the highest present value of flood reduction benefits from mangroves. Using high resolution structure data and building-specific damage curves, we estimate the present value of Florida mangroves for flood protection as \$50 billion (using a 4% discount rate). The average benefit-cost ratio (BCR) of mangrove restoration for flood risk reduction across the entire wider Caribbean was 0.3 (at a 4% discount rate over 30 years): some of the highest average BCRs were obtained in Mexico (1.47), The Bahamas (1.52) and Florida (0.36).



Table of Contents

1. Introduction	1
2. Methods	3
2.1. Methods overview	3
2.2. Study site and coastal segmentation	4
2.3. Coastal flood modeling	4
2.4. Socioeconomic exposure, damage, and risk	6
2.5. Mangrove fragility curves	8
3. Data	12
3.1. Climate data	12
3.2. Habitat data	13
3.3. Bathymetry and topography data	13
3.4. Socioeconomic data (Caribbean wide)	14
3.5. Socioeconomic data (Florida)	15
3.6. Cost of mangrove restoration	16
3.7. Present Value and Benefit to Cost Ratios	17
4. Results	19
4.1. Caribbean-wide analysis of Present Value, BCR of mangrove restoration for flood reduction and Annual Expected Benefits to people (5-km study units)	19
4.2. Florida: High resolution assessment of economic risks and mangrove benefits	25
4.3. Using fragility curves to assess likelihood of mangrove loss to storms	29
5. Discussion	32
6. Conclusion	35
Literature cited	36

1. Introduction

Ecosystems provide benefits that society should account for, but these services are rarely valued rigorously, spatially, and most importantly in the economic terms needed by investors and government agencies (Bresch et al., 2010; Reguero et al., 2018). The limited data on the benefits provided by ecosystems and the cost to restore them has been identified as a major impediment in the advancement of ecosystem-based adaptation; Nature-based Solutions; and Natural and Nature-Based Features (FEMA, 2020; USACE 2021; IPCC 2019).

While mangroves are one of the most severely degraded marine ecosystems, our ability to restore these ecosystems at scale has increased significantly over the past two decades. However, there is little rigorous information regarding how to finance and where to focus these restoration efforts. A recent study suggests that global investment in the resto-

ration of mangroves could return \$11.8 billion by 2040 (Earth Security Group 2021).

Coastal ecosystems such as reefs and mangroves act as natural barriers to waves and storm surge, reducing flood damages to people and property. They also provide other co-benefits such as carbon sequestration or food provisioning. These benefits are critical across the Caribbean, where there have been substantial increases in storm risk and extensive habitat loss over the past 30 years (Lange et al. 2021). To identify where mangrove restoration could yield significant Return on Investment (ROI), we build on recent work that rigorously values the annual flood risk reduction benefits of coastal habitats (Beck et al., 2018; Menéndez et al., 2020). We then combine these updated flood risk reduction benefits of mangroves with location-specific information on mangrove restoration costs to assess the cost-effectiveness of mangrove restoration and protection.



Mangroves along the coast of Warderick Wells Cay in The Bahamas Exuma Cays Land & Sea Park. © Mark Godfrey/TNC.

2. Methods

2.1. Methods overview

In this report we describe methods for assessing flood risk to coastal communities, the long-term benefits derived from mangrove presence, and the return on investment (ROI) of mangroves for flood risk reduction. Our core methods and results are based on the work in Menéndez et al. (2020) and Beck et al. (2022). We have substantially updated the data and results from Beck et al. (2020) by: (i) assessing risk and benefits at a fine scale (5-km study units) across the Caribbean; (ii) using very high resolution economic data for Florida from the U.S. National

Structure Inventory (NSI); (iii) applying comprehensive structure-specific flood depth damage curves from the U.S. Army Corp of Engineers (USACE) to the NSI data using the U.S. Federal Emergency Management Agency's (FEMA) Flood Assessment Structure Tool (FAST); and (iv) using new data on the costs of restoration across Mexico, Florida, and The Bahamas.

The core assessment in this report is on coastal flood risk and the value of mangroves for reducing this risk. The report follows approaches developed with the World Bank for assessing flood risk and the benefits of mangroves for risk reduction. We combine probabilistic analysis of storm hazards with process-based modelling of coastal flooding

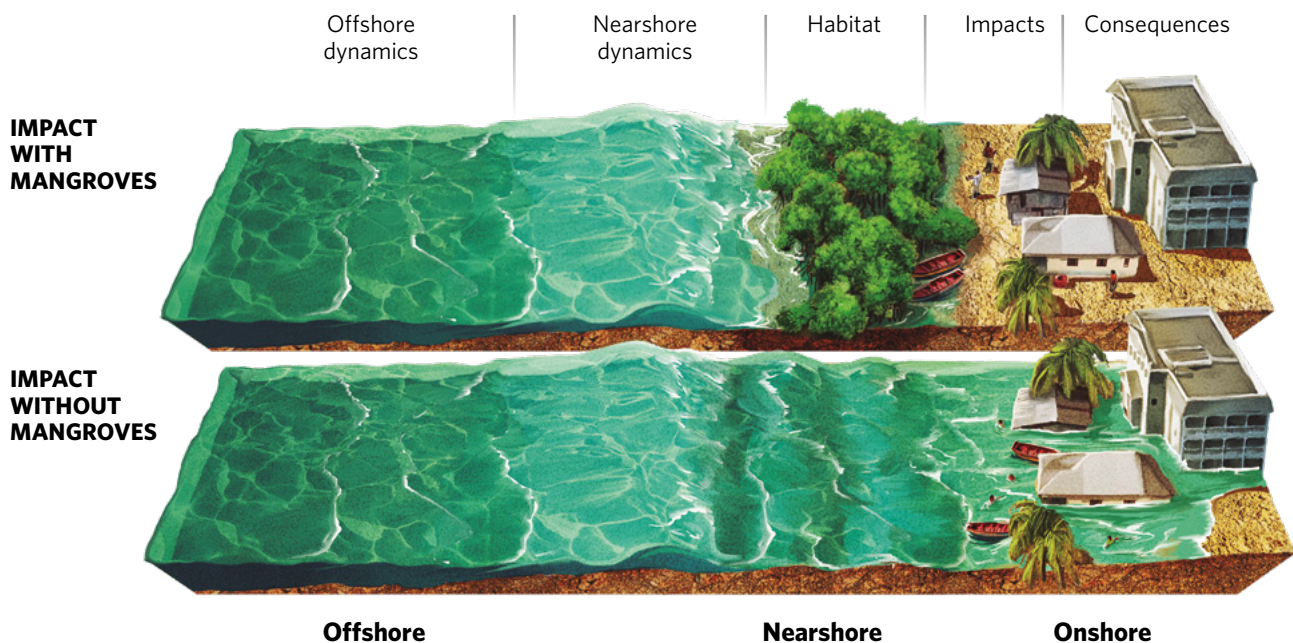


Figure 1: Key steps and data for estimating the flood protection benefits provided by mangroves. Step 1, Offshore dynamics: Oceanographic data are combined to assess offshore sea states. Step 2, Nearshore dynamics: Waves are modified by nearshore hydrodynamics. Step 3, Habitat: Effects of mangroves on waves and surge are estimated. Step 4, Impacts: Flood heights are extended inland along profiles (every 1 km) for 10-, 25-, 50-, and 100-year events, with and without mangroves. Step 5, Consequences: The consequences to land, people, and built capital are estimated. (Adapted from Beck et al. 2019) ©PuntoAparte.

and detailed exposure (people and property) data, with and without mangroves. We estimate flood extents and annual expected flood damages by assessing flooding events of multiple return periods (10-, 25-, 50-, and 100-year events). We examine flooding and socioeconomic exposure, with and without mangroves. Then, by following the Expected Damage Function approach (Beck et al., 2016), we estimate the flood protection benefits provided by mangroves based on the flood damages avoided to people and property by keeping mangroves in place (Figure 1).

These methods have been applied in several previous projects to assess the value of coral reefs for coastal protection globally (Beck et al., 2018) and to assess the value of mangroves for coastal protection in the Philippines, Jamaica, and globally (Losada et al., 2017; Menéndez et al., 2018; Menéndez et al., 2020; Ortega et al., 2019).

2.2. Study site and coastal segmentation

We assess flood risk and mangrove benefits across North America, with a focus on Mexico, Florida, and The Bahamas. The flood risk analysis is assessed on different spatial scales levels. The first level of analysis is at the local scale for consideration of the social and economic risk and benefits. In prior work we assessed risk and benefits in 20-km study units. We now assess risk and benefits at a substantially finer scale, i.e., in 5-km study units. These study units extend up to 30 km inland, 10 km seaward and along the coast for -5 km (Menendez et al., 2020). A second level of this analysis was conducted in Florida only, where higher resolution socioeconomic data is available, on point-level infrastructure and asset data, which were then summarized in administrative boundaries, e.g., Census Block Groups.

In total, 121,000 km of coastline, including more than 31,000 km² of mangroves (approximately 29% of the total global mangrove cover) were assessed across the Caribbean. We used cross-shore profiles 1 km apart to

model tropical cyclone driven waves and storm surge propagation. Each profile contains the following information: (i) profile slope (i.e., from mean water depth along the profile at multiple distance intervals from offshore to shoreline); (ii) height of coral reef; (iii) total height and width of mangroves. There are 2,170 profiles in Florida, 9,330 profiles in Mexico, and 3,542 profiles in The Bahamas.

2.3. Coastal flood modeling

2.3.1. Offshore dynamics

We used global offshore historical climate data (waves, storm surge, sea level, and tropical cyclones) to model offshore dynamics. The offshore dynamics are split into two different categories: high intensity events (tropical cyclones) and low intensity events (regular climate). Both conditions are modeled separately but they share some components such as the astronomical tide, which comes from the Global Ocean Tides data set (GOT, (Ray, 1999)), and mean sea level time series (from 1979 to 2010) at 100-km resolution. Other components, such as waves and storm surge, are computed separately under high intensity and low intensity events.

2.3.2. Nearshore propagation

Waves and storm surge driven by tropical cyclones are calculated seaward of the mangrove habitat, at the most offshore side of each cross-shore profile (head). We used the parametric model developed by Menéndez et al. (2020) to estimate wave height, wave period, storm surge, and storm duration produced by each of the tropical cyclones from IBTrACS database (Knapp et al., 2010) at the head of each cross-shore profile. The input variables in the parametric model are the minimum distance between the cyclone track and the target point; the maximum wind speed at the minimum distance location; the angle between the cross-shore profile and wind; and the average storm velocity. We assume that deep water ocean dynamics produced by any climate condition other than tropical cyclones are analyzed as regular climate.

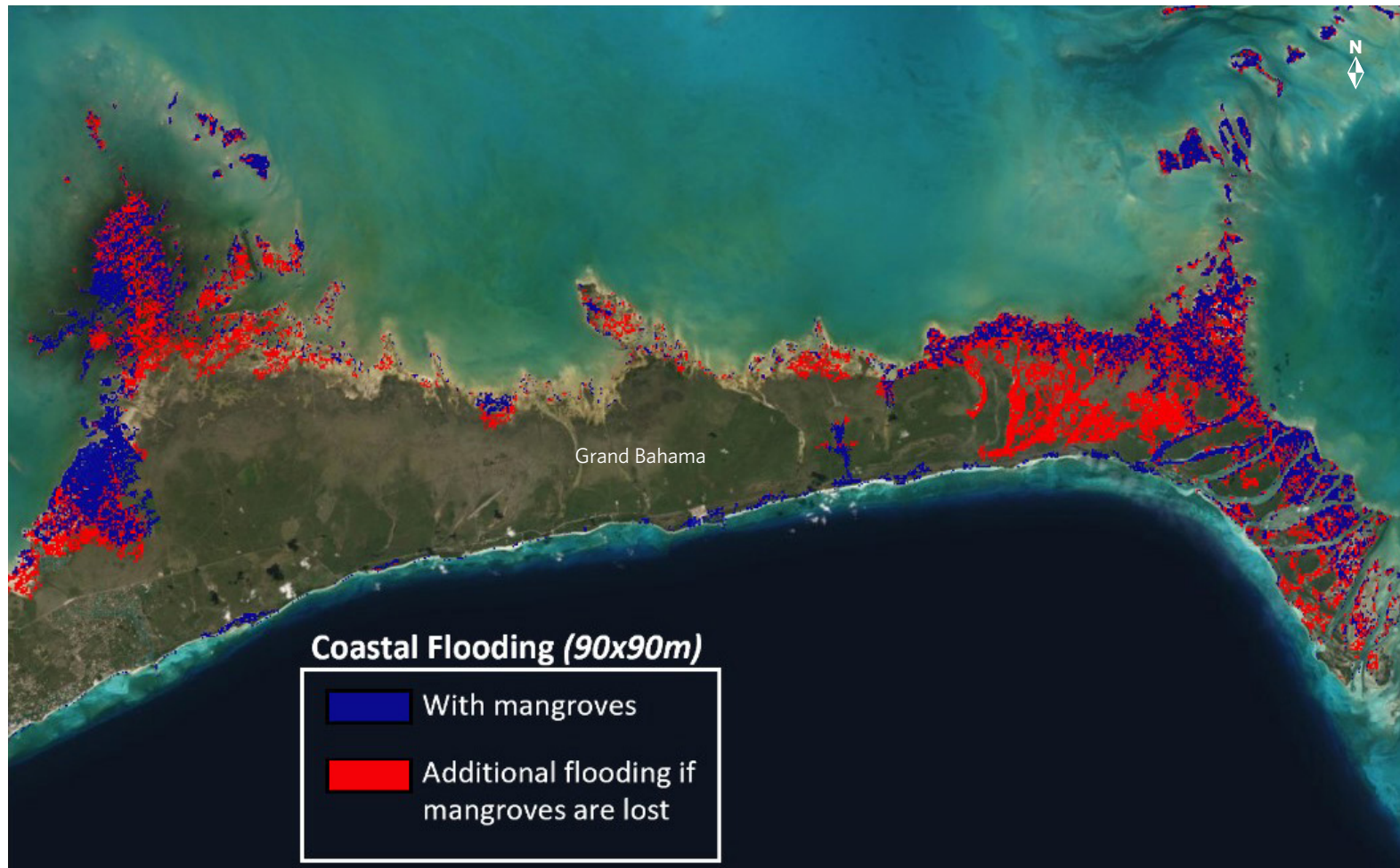


Figure 2: Flooded area in Grand Bahama Island (The Bahamas) for a 10-year flood event from tropical cyclones. Blue area represents the flood extent with current mangrove cover. Red area represents the additional flooding without mangroves.

2.3.3. Mangrove hydrodynamic modeling and flood height calculation

To transform waves and storm surge seaward of the habitat into the total water level at the shoreline (flood height), we need to account for the effect of mangroves and coral reefs on wave energy and surge dissipation. Flood height calculation is assessed using the relationship (i.e., look-up-tables) developed by Menéndez et al. (2020), where flow-habitat interaction is considered.

2.3.4. Flood extent calculation

To transfer the flood height into land, we used the GIS “bathtub” method. We used four return periods: 10, 25, 50 and 100 years. The minimum incidence rate is marked by the limitation of some areas with a shortage of extreme events, i.e., where there are no records of frequent flooding. We used a hydraulically-connected bathtub method to connect the points of the global Shuttle Radar Topography Mission (SRTM) topography (90 m horizontal resolution) that are below the water level. Figure 2 is an example of this fourth step of the methodology and shows coastal flooding produced by tropical cyclones in The Bahamas for a 10-year event.

2.4. Socioeconomic exposure, damage, and risk

2.4.1. Caribbean-wide resolution: Joint Research Centre damage functions

The assessment of the consequences (risk) of the loss of mangroves was measured in terms of people and property damaged. Throughout this report, we used stock and property interchangeably to mean the physical buildings. Flood risk is the intersection of the impact (flooding), exposure (population and property

in the flood plain area), and vulnerability (damage by water depth level). We used the population data in the Gridded Population of the World (GPW) from the Socioeconomic Data and Applications Center (SEDAC) at 1-km resolution and the distribution of residential and industrial stock from the Global Assessment Report (GAR15) at 5-km resolution. Population and stock data were resampled to 90 m square pixels to match with the flood layers distribution. We intersected the flood layer and the socioeconomic data to identify people and stock flooded at 90 m resolution.

We used depth-damage functions to quantify the losses that would occur at various water depths to population and stock (Figure 3). Population damage is based on the hypothesis that water depths below 0.5 meters do not affect people, while water depths above 0.5 meters affect 100% of people flooded. Often damage functions are not applied to estimate people impacted by flooding (Hinkel et al., 2014). This option, however, overestimates the people impacted, and it is recommended to identify the flooding thresholds below which the impacts of flooding to people are negligible (Hallegatte et al., 2013). We set

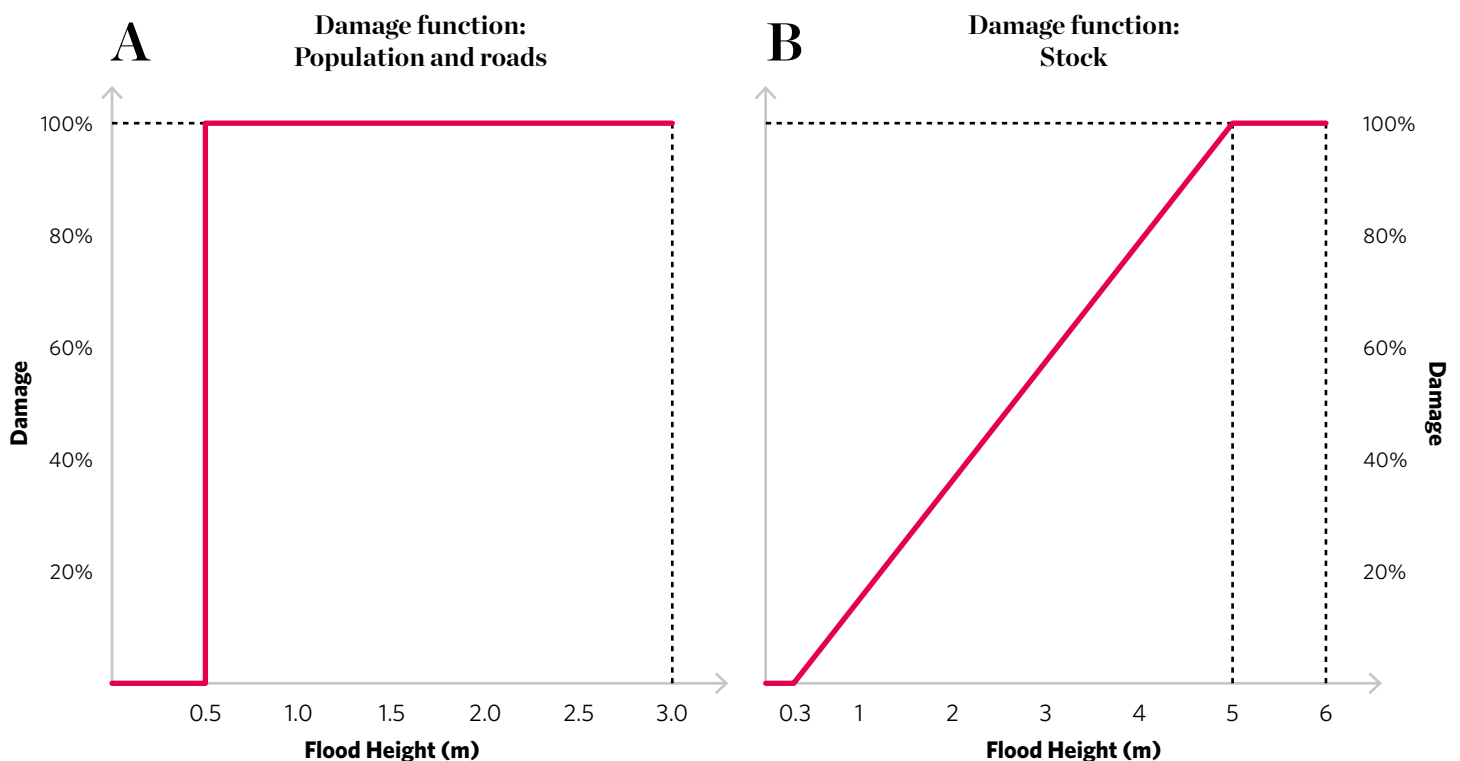


Figure 3: Generalized depth damage curves used throughout the Caribbean where data on structure types and country-specific damage curves were not available.

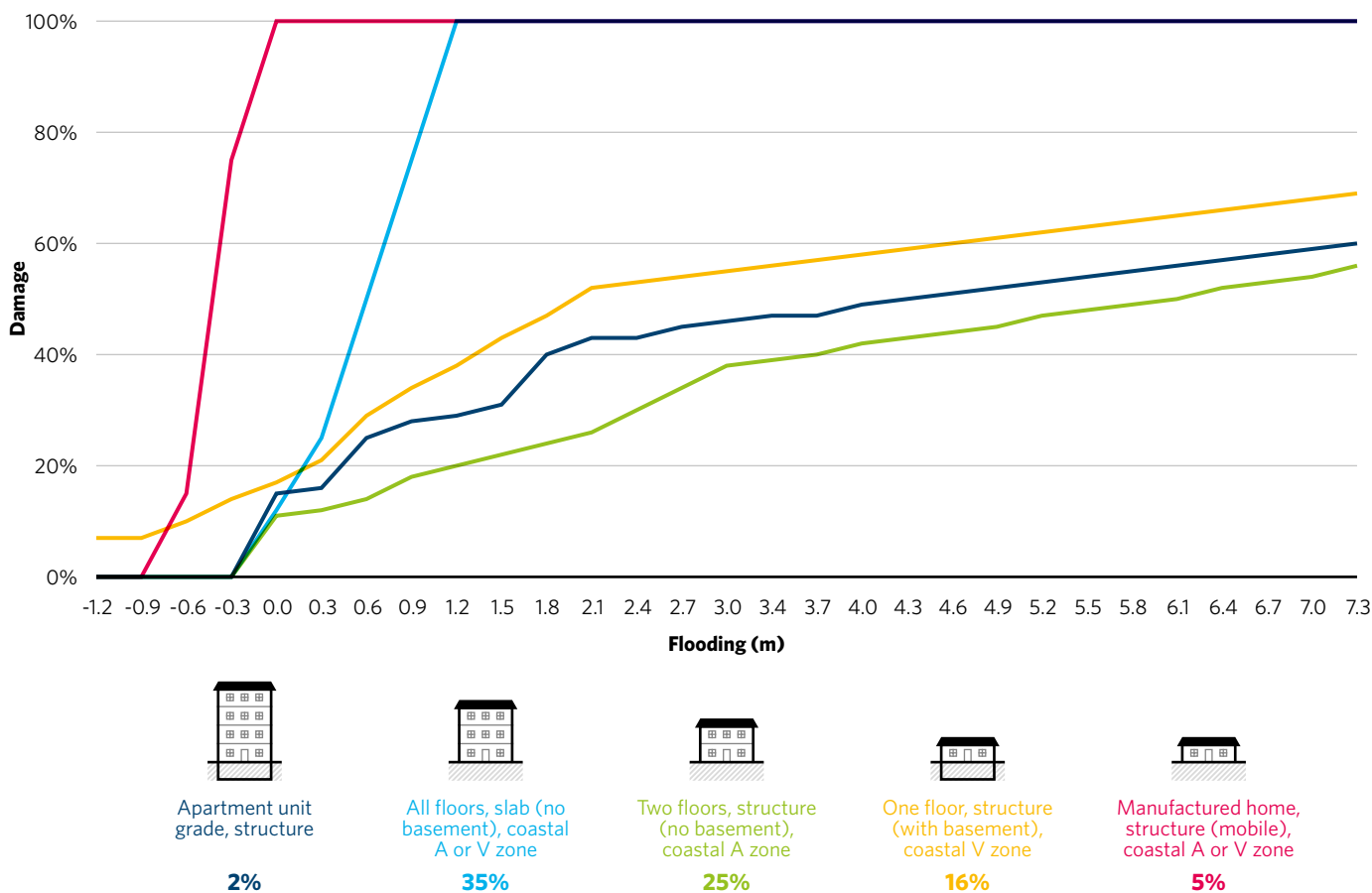


Figure 4: FEMA FAST/USACOE Depth Damage Functions. The flood depth-damage curves associated with the five most common structure types flooded in the Florida project area. The percent values below each building type represent the percent of total flooded structure represented by each structure type. While 34 structural types were flooded across all storm scenarios, these five building types represent 83% of the sample.

this threshold at 0.5 m, which is a common value used by emergency services (Japan, Netherlands, U.S.) in determining when it is necessary to evacuate people. In the case of stock, we adapted the “Global Flood Depth-Damage Functions” from the Joint Research Centre (JRC) broken down by continent (Africa, Asia, Oceania, North America, South America and Central America) (Huizinga et al., 2017).

The combination of damage curves and the distribution of people and stock exposed to flooding gives us the consequences for various severities of flooding, defined here by return period. We then derived the Expected Annual Values of flood. We integrate flood risk and mangrove benefits by return period in the 5-km study units across the region.

2.4.2. Florida: High resolution assessment of economic risks and mangrove benefits

In Florida, we did high resolution assessments of flood risk and mangrove flood reduction benefits using data from the NSI and USACE damage curves included in the FEMA FAST (Figure 4). NSI includes point-level asset data, which allows for economic calculations at very high resolution. In the Florida project area (i.e., Florida coasts with mangroves), there were 34 different building types in the NSI database and each structure type was matched with a specific flood depth-damage curve.

2.5. Mangrove fragility curves

In the engineering and insurance sector, fragility curves reflect the probability of exceeding various levels of structural damage—from no damage to complete structural failure—from natural hazards such as earthquakes and storms. For mangroves, we reviewed the literature for data that could be used to describe their likelihood of failure during storm events, i.e., their fragility curve. From an insurance perspective, these fragility curves are important for two reasons. First, they can be used to adjust predictions of flood risk and mangrove benefits. If mangroves fail in extreme events, the flood risk will increase above predicted levels and the predicted benefits from mangroves will decrease. Second, storms are a major source of mangrove loss and this natural asset can be insured against these losses once these failure rates can be reasonably identified and measured. This second reason is the basis of the insurance for coral reefs in Mexico (Beck et al., 2019; Secaira et al., 2019). In this section we describe the methods to estimate the annual expected mangrove loss in the Caribbean region, by building synthetic tropical cyclone data and implementing mangrove loss rates present in the literature.

Wind speed is directly correlated with mangrove loss. Two studies have assessed the changes in mangrove extent after tropical cyclones in Florida and the Caribbean (Han et al., 2018, Taillie et al., 2020). Hurricane-induced losses of mangrove habitat were assessed across the Everglades National Park Mangrove Forest over several decades (Han et al., 2018) and across the Caribbean over the severe hurricane season in 2017 (Taillie et al., 2020).

Taillie et al. (2020) also used a remote sensing analysis to assess the relationship between storms and mangroves, but over a more limited time frame. They used an indirect measure of habitat change based on the Normalized Difference Vegetation Index (NDVI). NDVI quantifies vegetation by measuring the difference between near-infrared (which vegetation strongly reflects) and red light (which vegetation absorbs). They assumed that mangroves were damaged if the index score dropped by 0.2 following a storm.

The fragility curves developed from this NDVI approach are focused more on vegetation damage and less on the overall loss of mangroves. Their NDVI based curves suggest major impacts to mangroves during even modest hurricanes (Taillie et al., 2020). For example, they predict that ~25% of mangroves would be damaged if maximum wind speed reached just 100 km/h (i.e., less than a Category 1 hurricane). In our experience, this prediction represents a very high estimate of mangrove loss from frequent events.

Han et al. (2018) assessed mangrove habitat loss and recovery from several hurricanes over time. They used a relatively direct measure of habitat loss and gain across multiple time periods before and after major hurricane events. We used Han et al. (2018) to extract the mangrove damage values from the chart (Figure 5) and developed a regression to describe the fragility curve (Equation 1).

We then ran an example assessment of how the data from the fragility curve could be coupled with location-specific wind speeds to identify the likelihood of damages to mangroves across Mexico, Florida, and The Bahamas. We recognize that environmental and hazard managers and in particular insurers might use their own wind speed data to update this assessment.

We estimated the annual expected mangrove loss at different locations across the Caribbean by developing a large sample of historic tropical cyclones passing through the study area. The historical storms database alone, based on IBTrACS v4, did not include enough events for an accurate probabilistic assessment of wind speed. Therefore, we developed a stochastic simulation of the historical tropical cyclones (TC) to increase the sample size from 170 years (1851-2020, including 1,140 storms) up to 1,000 years (including 6,635 storms). We used the TCWiSE model from Deltares (Nederhoff et al., 2021). The TCWiSE model simulates synthetic tropical cyclone tracks for statistically reliable wind and pressure estimations. The tool uses the method of Empirical Track Modelling (ETM) to generate the synthetic cyclone tracks from their genesis to termination points with 3-hourly intervals. The cyclone track is determined by the coordinates of the cyclone eye, the heading, and forward speed. The cyclone intensity is determined by maximum sustained wind speed. This results in a set of synthetic tropical cyclones with the di-

rection of the track, the forward speed and the maximum sustained wind speed at each time step. When a tropical cyclone is over land, the maximum sustained wind speed decreases exponentially based on Kaplan and DeMaria (1995). Overall, there is good agreement with the spatial distribution of tracks between the observational record (IBTRACS V4) and the TCWiSE model (Figure 5).

Because local wind speed will have a direct effect on mangrove damage, we combined study units into subregions (Figure 6) and analyzed the tropical cyclone activity in each. We divided Florida into 11 subregions, Mexico into 6 subregions, and The Bahamas into 10 subregions.

We calculated the maximum wind speed of synthetic storms crossing each of the subregions. Time series of 1,000 years long of maximum wind speed were reconstructed for each subregion.

Given maximum wind speed time series, we applied the regression formula (Equation 1) to calculate the time series of mangrove damage. Then we fitted the data to a Pareto-Poisson distribution to obtain the percent of mangrove loss per return period in each subregion. Finally, we integrated the curve across all return periods to obtain the annual expected percent of mangrove loss. The full methodology is described in Figure 7.

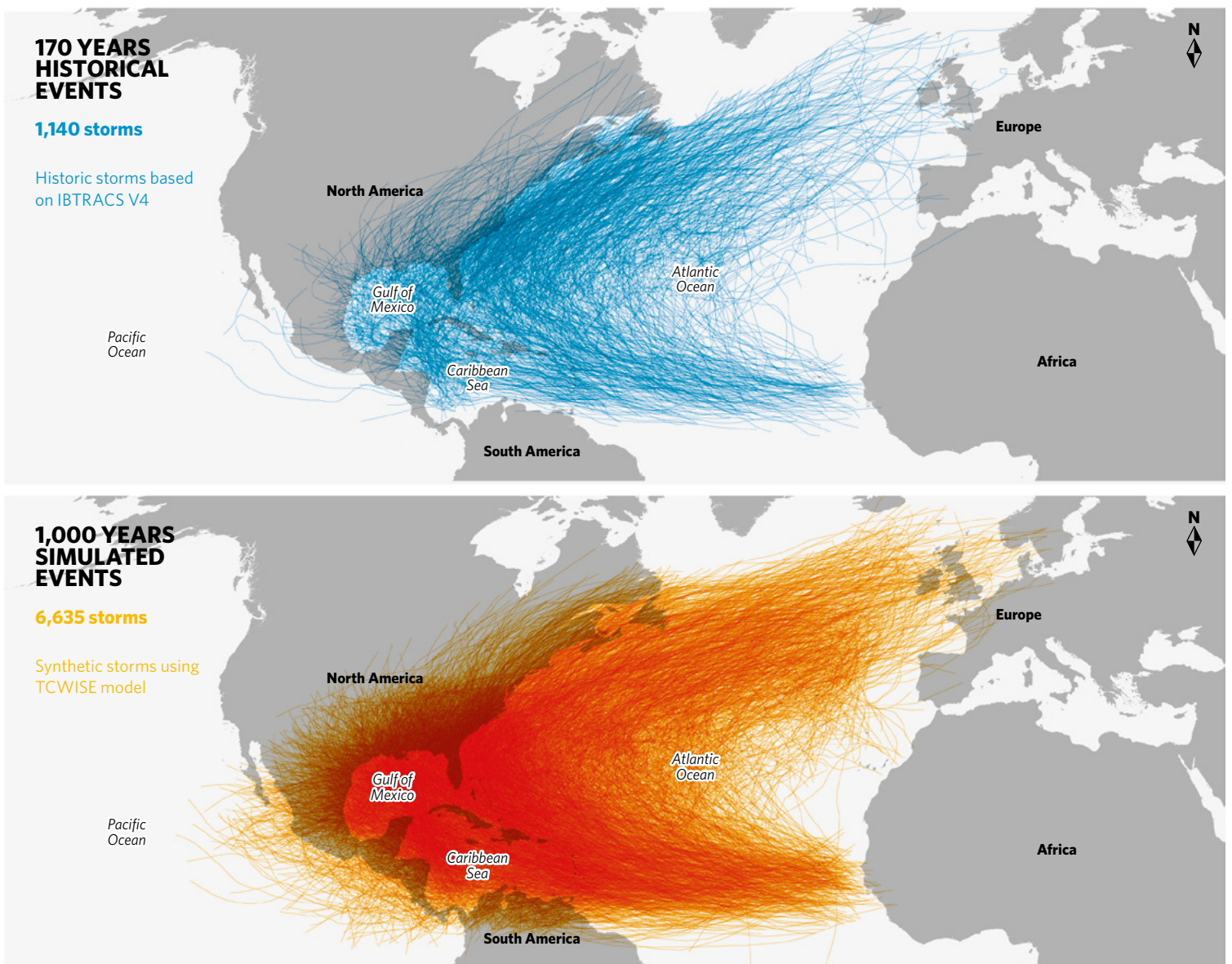


Figure 5: Historic tropical cyclones based on IBTrACS V4 (top panel) versus synthetic tropical cyclones generated with TCWiSE model (bottom panel).



A boat glides through coastal mangroves in the Reserva de la Biosfera la Encrucijada near the town of Salto De Agua, Chiapas, Mexico. © Mark Godfrey/TNC.



Figure 6: Subregions used to analyze mangrove fragility and expected mangrove loss.

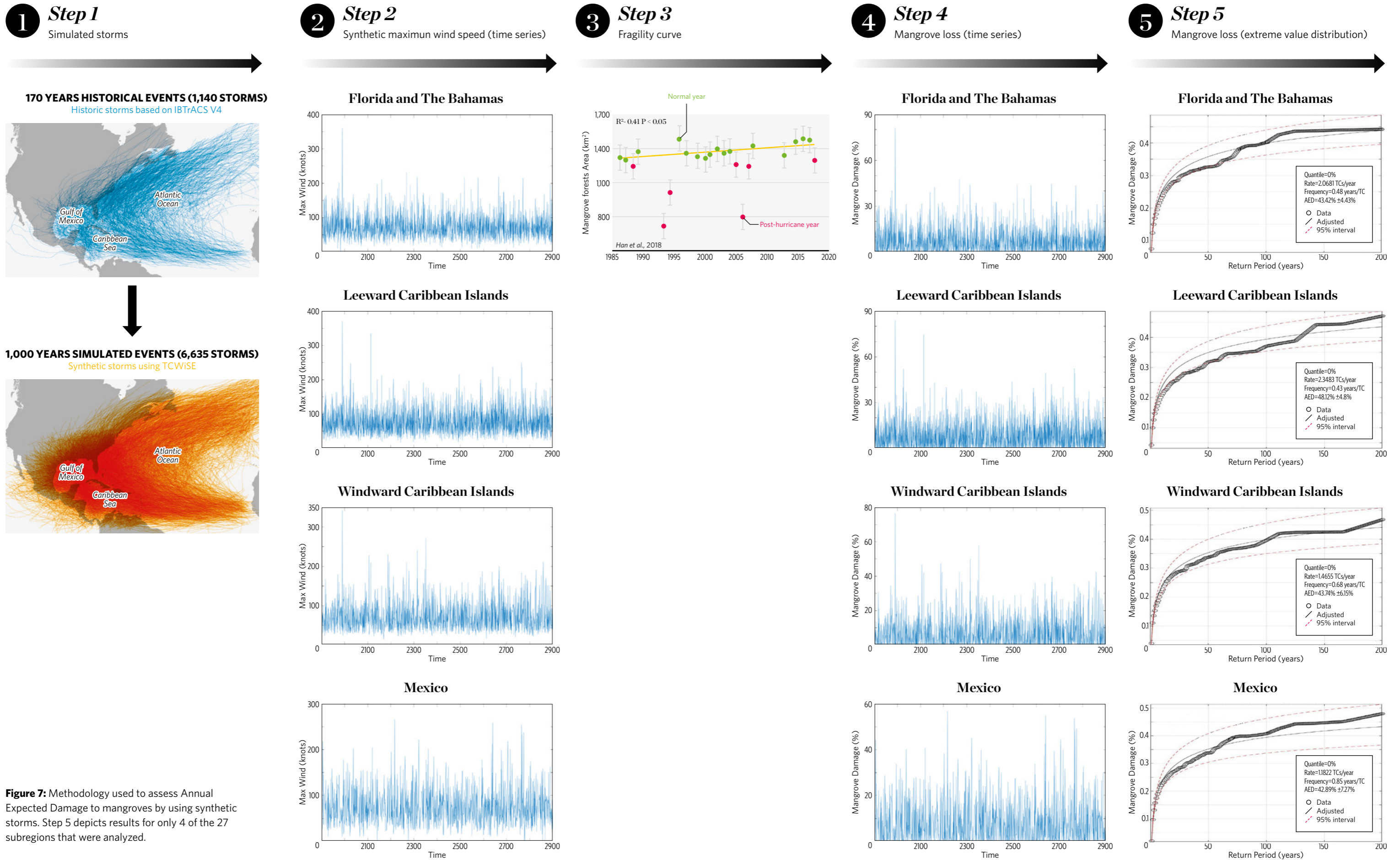


Figure 7: Methodology used to assess Annual Expected Damage to mangroves by using synthetic storms. Step 5 depicts results for only 4 of the 27 subregions that were analyzed.

3. Data

3.1. Climate data

3.1.1. Tropical cyclones

The data sets on tropical cyclones and waves provide locally specific information from more than 7,000 historical cyclones globally (Knapp et al., 2010). The International Best Track Archive for Climate Stewardship (IBTrACS) data set contains 6-hour information on tropical storms (winds between 63 km/hour and 119 km/hour) and tropical cyclones (winds above 119 km/hour) in different ocean basins (<ftp://eclipse.ncdc.noaa.gov/pub/ibtracs/v03r10/all/shp/>). Each tropical storm is characterized by maximum wind speed at the eye of the storm (wind max) and track evolution with time (Lon, Lat, Time). The IBTrACS database includes information from different regional, national, and international agencies (e.g., NOAA, Japan, and Australia meteorological agencies). The heterogeneity of the data sources that feed into IBTrACS database produce high variability in the temporal and spatial coverage across ocean basins. Tropical cyclone data at the North Atlantic basin starts in 1855.

3.1.2. Waves

Waves under regular climate conditions (low intensity events) are obtained from the new global reanalysis GOW 2 (Global Ocean Waves, Perez et al., 2017), an update of GOW 1, (Reguero et al., 2012) that increases the accuracy of extreme events. GOW 2 provides hourly data of waves from 1979 to 2016 globally at 0.25° resolution. It contains historical time series of wave height (Hs), wave period (Tp, Tm) and wave direction (Dp, Dm). The authors used the WaveWatch III model (Tolman, 2014) forced with a global atmospheric reanalysis CFSR (Climate Forecast System Reanalysis), from NCEP (National Centers for Environmental Prediction) Climate Forecast System Reanalysis (Saha et al., 2010).

Wave time series were validated with buoys and satellite data. In case of tropical cyclone conditions, waves are calculated nearshore by using the parametric formula from Menendez et al. (2020).

3.1.3. Storm surge

Storm surge data under regular climate conditions are derived from the reanalysis series created from the Dynamic Atmospheric Correction (DAC) and from the pressure fields of the NOAA-CIRES Twentieth Century Reanalysis Project (Compo et al., 2011). The DAC database provides an hourly time series of storm surge data from 1871 to 2010 at 2° resolution globally (Cid et al., 2017). These data lack temporal and spatial accuracy to capture storm surge driven by tropical cyclones. Therefore, storm surge produced by tropical cyclones is calculated in the same way as waves, by using the storm surge formula from Menendez et al. (2020).

3.1.4. Astronomical tide

The astronomical tide is obtained from the Global Ocean Tides (GOT) database, with a resolution of 25 km and time length from 1900 to 2100 (ihdata@ihcantabria.com). It includes an hourly time series of sea surface elevation driven by the gravitational interaction between the Earth, moon, and sun.

3.1.5. Mean sea level

The data set of historical time series of mean sea level (from 1950 to 2010) includes observations on variations in mean sea level on a monthly basis at a scale of 100 km (Church et al., 2004). TOPEX/Poseidon satellite altimeter data are used to estimate global empirical orthogonal functions that are then combined with historical tide gauge data.

3.2. Habitat data

3.2.1. Mangroves

This study uses one global data set for mangrove cover—the Global Mangrove Partnership Data, which was created in 2010 for the World Atlas of Mangroves (Spalding, 2010) and covers 98.6% of all mangrove forests. These data show the global distribution of mangroves, and was produced as a joint initiative of the International Tropical Timber Organization (ITTO), International Society for Mangrove Ecosystems (ISME), Food and Agriculture Organization of the United Nations (FAO), United Nations Environment Programme World Conservation Monitoring Centre (UNEP-WCMC), United Nations Educational, Scientific and Cultural Organization’s Man and the Biosphere Programme (UNESCOMAB), United Nations University Institute for Water, Environment and Health (UNUINWEH) and The Nature Conservancy (TNC). Major funding was provided by ITTO through a Japanese Government project grant and the project was implemented by ISME.

3.2.2. Coral reefs

We used global distribution data of coral reefs (Spalding, 2010), which was updated by Burke et al. (2011). These data provide spatial distribution of reefs, but they do not include bathymetry. We associated a friction coefficient to the Caribbean coral reefs based on the conservation status of coral reefs (Nunes & Pawlak, 2008) and the friction coefficient table of Sheppard et al. (2005). We used a friction coefficient of 0.14 along the Caribbean. The water depth at the reef crest was obtained from Sea-Viewing Wide Field-of-View Sensor (SeaWiFS) bathymetry (<https://oceancolor.gsfc.nasa.gov/cgi/reefs.pl>), which has been specifically developed in coral reef areas globally (Robinson et al., 2000).

3.3. Bathymetry and topography data

Collecting good bathymetry and topography data is critical for these type of flooding analyses (Beck et al., 2022; World Bank, 2016). The availability and quality of bathymetry and topography data sets varies greatly across the world. We aimed to use the best available global data to reduce uncertainty in the coastal protection valuation.

Accurate bathymetry of shallow nearshore coral reefs in tropical countries is critical for predicting flooding because the reefs help dissipate wave energy, resulting in less wave energy reaching mangrove shorelines. With a spatial resolution of 1 km, SeaWiFS bathymetry is the most accurate database for coral reef bathymetry globally. Therefore, for bathymetry, we combined SeaWiFS with the General Bathymetric Chart of the Oceans (GEBCO) 1:1.6 km resolution (1 arc min) global topobathy database to obtain a hybrid mesh with high quality water depth values nearshore.

Adequate flooding analyses require high resolution topography data, or a Digital Terrain Model (DTM). For topography, we used the Shuttle Radar Topography Mission (SRTM), which at 90x90m horizontal resolution, which was the best available DTM global elevation data.

3.4. Socioeconomic data (Caribbean wide)

3.4.1. Property data

We estimated the property value in the floodplain area as the sum of two spatial distributions of stock (industrial and residential). The spatial distribution of residential and industrial stock are from the Global Assessment Report on Disaster Risk Reduction database (GAR15) (Desai et al., 2015) and is at a spatial resolution of 5 km worldwide, with a 1 km detailed spatial resolution in coastal areas. The GAR15 data is based on 2010 economic data from the World Bank Changing Wealth of Nations report (De Bono & Chatenoux, 2015). The variables included in the database are number of residents and economic value of residential, commercial, and industrial buildings (De Bono & Chatenoux, 2015). The GAR15 database follows a top-down approach using geographic distribution of population and gross domestic product (GDP) as proxies to distribute the rest of the socioeconomic variables (e.g., income, education, health, building types). These national-level variables on socioeconomic characteristics, building type, and capital stock are transposed onto 5x5 km or 1x1 km grids (UNISDR 2015). The study downscaled residential and industrial stock data from the GAR15 in the following manner:

1. For each point of the GAR15 layer, the total population was calculated. Eight fields were added together: high, medium high, medium low and low income for both rural and urban populations.

2. In each point of the GAR15 layer, total residential building stock was calculated. Eight fields were added together: high, medium high, medium low and low income for both rural and urban residential stock.
3. In each point of the GAR15 layer, residential stock per capita was calculated by dividing residential stock by adjusted population.
4. A raster layer was created for residential stock per capita. Inverse distance weighted interpolation was used for the creation of this raster.
5. Finally, using the population raster from WorldPop (100 m resolution) the residential raster layer was calculated by multiplying residential stock per capita and population (Tatem 2017). A scale verification was done, checking that the sum of residential stock from the GAR15 layer was the same as the sum of residential stock raster layer created. Industrial stock data were downscaled similarly.

3.4.2. Damage functions: JRC

The sensitivity of people and stock to different levels of flooding was obtained through damage functions (Figure 3). Damage functions provide information on assets affected by coastal flooding as a function of water depth. For stock, we adapted the “Global Flood Depth-Damage Functions” from JRC broken down by continent and by asset type: residential and industrial (Huizinga et al., 2017).



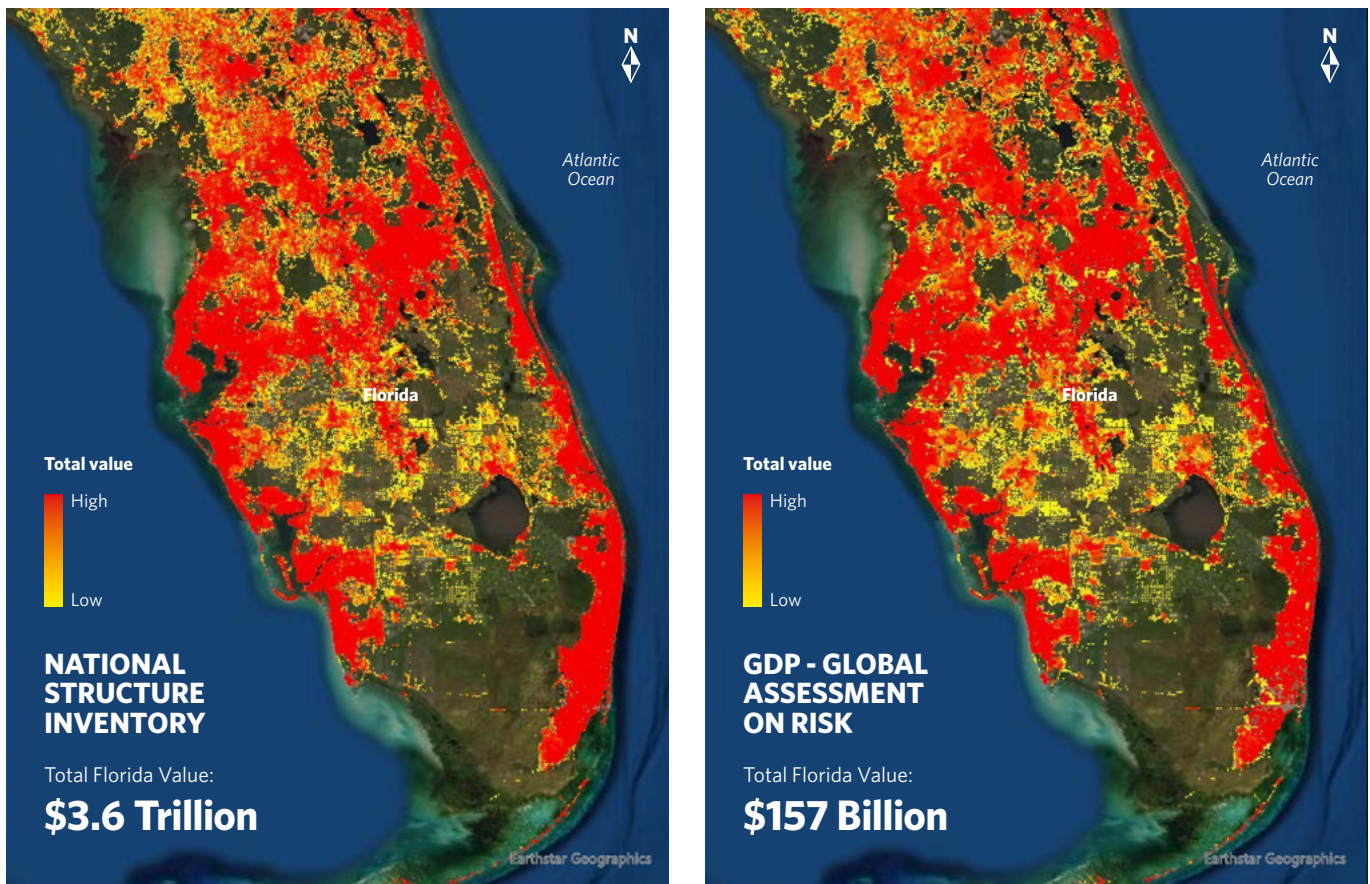


Figure 8: Comparing Asset Data in National Structure Inventory (NSI) and GDP-Global Assessment on Risk (GAR). There is high correlation in the spatial distribution of economic assets in these two databases ($r=0.78$). However, the overall values are significantly different, with NSI identifying much greater total value in Florida. Both datasets are displayed at GAR's native 1 km resolution and shown with 10 category quantiles.

3.5. Socioeconomic data (Florida)

3.5.1. Property data: NSI

The existence of high-resolution asset data in Florida allowed for the calculation of risk at the building level. We used the NSI to calculate risk to over 7 million individual structures across Florida. In addition to high spatial accuracy and reasonable completeness, NSI includes attributes that allow for more specific application of structure-specific depth-damage curves. A comparison of the total values and spatial distribution of values in NSI and GAR is shown above (Figure 8).

3.5.2. Damage functions: FEMA FAST

The Flood Assessment Structure Tool (FAST) is a FEMA tool for evaluating expected building and content value loss as a function of flood depth. When used in conjunction with the structural attributes of NSI, it allows for the application of depth-damage functions from USACE that are structure-specific, leading to a more accurate loss calculation.

For each storm return period, NSI data was run through FAST, calculating expected loss on a per-building level. The point-level asset data was then aggregated into meaningful geographies, including 5-km study units and Census Block Groups. Annual Expected Benefit was calculated using the methodology in Menendez (2020).

3.6. Cost of mangrove restoration

In this report, we describe the costs of mangrove restoration across the wider Caribbean region, with a particular focus on Mexico, Florida, and The Bahamas. TNC provided mangrove restoration costs in Mexico, Florida, and The Bahamas based on location-specific mangrove restoration case studies and literature reviews (Herrera-Silveira et al., 2022). We used location-specific mangrove restoration costs for these three areas and another value to assess BCRs across the remainder of the study region.

Mangrove restoration costs in Florida were divided into two regions: western and eastern Florida. Eastern Florida covers the coastline from Jacksonville to Miami and includes all of the Florida Keys. Western Florida includes the coastline from the Ten Thousand Islands area north to Tampa. The highest mangrove restoration costs were reported in eastern Florida. The median restoration cost

of the 16 projects included in the analysis for eastern Florida was \$118,524 per hectare. The 27 projects in western Florida resulted in a median value of \$54,653 per hectare. In Mexico, 16 projects were considered, with a median restoration cost of \$4,538 per hectare. The median cost in the Bahamas across 5 projects was \$35,955 per hectare. The summary of all the mangrove restoration costs is included in Table 1.

In addition to the values provided by TNC, previous studies assessed data on restoration costs from 72 projects in the Caribbean (Narayan et al., 2019). These data were obtained through a systematic literature review of the reported costs of mangrove restoration projects in the region. This analysis was an extension of other reviews conducted by Bayraktarov et al. (2016) and Narayan et al. (2016). All costs were calculated per hectare. The median mangrove restoration cost in all other Caribbean regions was \$23,000 per hectare.

There are several factors that determine the costs of mangrove restoration projects, and costs per hectare are typically lower for larger restoration projects. In general, the factors influencing the costs of mangrove restoration projects are: (i) the costs of land and permitting; (ii) the

	Mexico	Western Florida	Eastern Florida	The Bahamas	All Other Caribbean
High 75th percentile	\$9,942	\$115,098	\$198,720	\$53,843	-
Low 25th percentile	\$1,865	\$13,659	\$70,941	\$33,097	-
Median	\$4,538	\$54,653	\$118,524	\$35,955	\$23,000

Table 1: Mangrove restoration costs in Mexico, Florida, and the Bahamas (in 2020 USD per hectare). High values correspond to the 75th percentile or above and low values correspond to the 25th percentile or below. Source: Herrera-Silveira et al., 2022 and Narayan et al., 2016.

costs of obtaining and transporting the material; (iii) the costs of designing and constructing the project, and; (iv) the costs of monitoring and maintaining the project post-construction (Narayan et al., 2019). Since mangrove restoration happens in the intertidal zone, the availability and price of land and the necessary permits are an important factor influencing costs. Another factor that influences costs is the restoration technique. Restoration by planting mangrove saplings can be cheap particularly if these projects also make use of local, voluntary labor. Projects involving hydrological restoration can be more expensive due to the need for specialized equipment, labor, and the purchase and transportation of sediment. Maintenance and monitoring are also important cost components, though often not reported in restoration projects. We find that specific maintenance actions, such as fencing restoration sites to reduce disturbance can significantly add to overall project costs (Narayan et al., 2019).

3.7. Present Value and Benefit to Cost Ratios

In this analysis, we estimated the Present Value of mangroves across the wider Caribbean region at the 5 km level. The countries and states that it was possible to include in the full analyses were Mexico, Florida, The Bahamas, Belize, Cuba, Dominican Republic, Jamaica,

Anguilla, Antigua and Barbuda, Colombia, Costa Rica, Dominica, Grenada, Guatemala, Haiti, Honduras, Nicaragua, Panama, Santa Lucia, Trinidad and Tobago, Turks and Caicos, U.S. Virgin Islands, and Venezuela.

We calculate the Present Value of mangroves as the sum of Annual Expected Benefits over a 30-year project lifetime using a discount rate of 4% or 7%. The BCR reflects the overall relationship between the costs of a proposed mangrove restoration project and the anticipated flood protection benefits (or future avoided losses).

To estimate restoration benefits, we assume that future restoration benefits will be similar to current flood risk reduction benefits per hectare within each study unit. This assumption is conservative because it applies the average value of benefits for all mangroves in a study unit. In reality, a mangrove restoration project for flood risk reduction would be sited and designed to maximize flood risk reduction (or at least perform better than average) in a study unit.

Using data on mangrove benefits (Present Value) and restoration costs, we calculated BCR for each study unit. In addition, we calculated mangrove benefits per hectare for each study unit. We mapped the data in ArcGIS to visualize spatial differences in BCR and PV per hectare.

We assume that mangrove restoration projects represent a 30-year coastal infrastructure asset. We apply two different discount rates across this project lifetime: 4% and 7%. Four percent is consistent with values we are using on project assessments with the World Bank. Seven percent is consistent with recommended discount rates for FEMA projects.



A mangrove outbreak under the Milky Way fights to survive desertification in the north of Quintana Roo, Mexico. © Carlos Gustavo Blanco Matus/TNC Photo Contest 2021.

4. Results

4.1. Caribbean-wide analysis of Present Value, BCR of mangrove restoration for flood reduction and Annual Expected Benefits to people (5-km study units)

We estimated the Present Value of mangrove assets and compared these benefits to potential costs of restoration across the Caribbean. We provide graphs and maps of the key results at the 5 km level across the region and then summarize the key results by country in Table 2.

4.1.1. Flood damage by storm

Present Value and BCR are based on the Annual Expected Benefits of mangroves. For a better understanding of the flood protection service across different storm scenarios, we show economic losses with and without mangroves under four return periods (10-, 25-, 50-, and 100-year event). In western Florida, damages with and without mangroves increase at the same rate as the return period increases (Figure 9, a), which means that mangroves provide almost the same protection for different storm events. Conversely, in eastern Florida mangroves provide greater benefits under the most intense storm conditions (Figure 9, b), same as in The Bahamas (Figure 9, d) and Mexico (Figure 9, c), where benefits are more remarkable under the most extreme events.

4.1.2. Present Value of mangroves

The mean 30-year Present Value per hectare of mangroves across the wider Caribbean within 5-km study units was \$8,094 per hectare, at a 4% discount rate (Figure 10 and Table 2). The total Present Value of mangroves across the Caribbean is \$25.17 billion. The top five regions in terms of Present Value of mangroves for flood protection are Mexico (\$6.26 billion), Florida (\$13.10 billion), The Bahamas (\$2.29 billion), Cuba (\$1.24 billion), and Guatemala (\$0.42 billion).

Among the three focal areas, The Bahamas presents the highest mean Present Value per hectare (\$54,570) followed by Florida (\$34,680) and Mexico (\$6,659). However, there are four other countries where the mean Present Value per hectare of mangroves exceeds \$10,000: Antigua and Barbuda, Jamaica, Guatemala and US Virgin Islands.

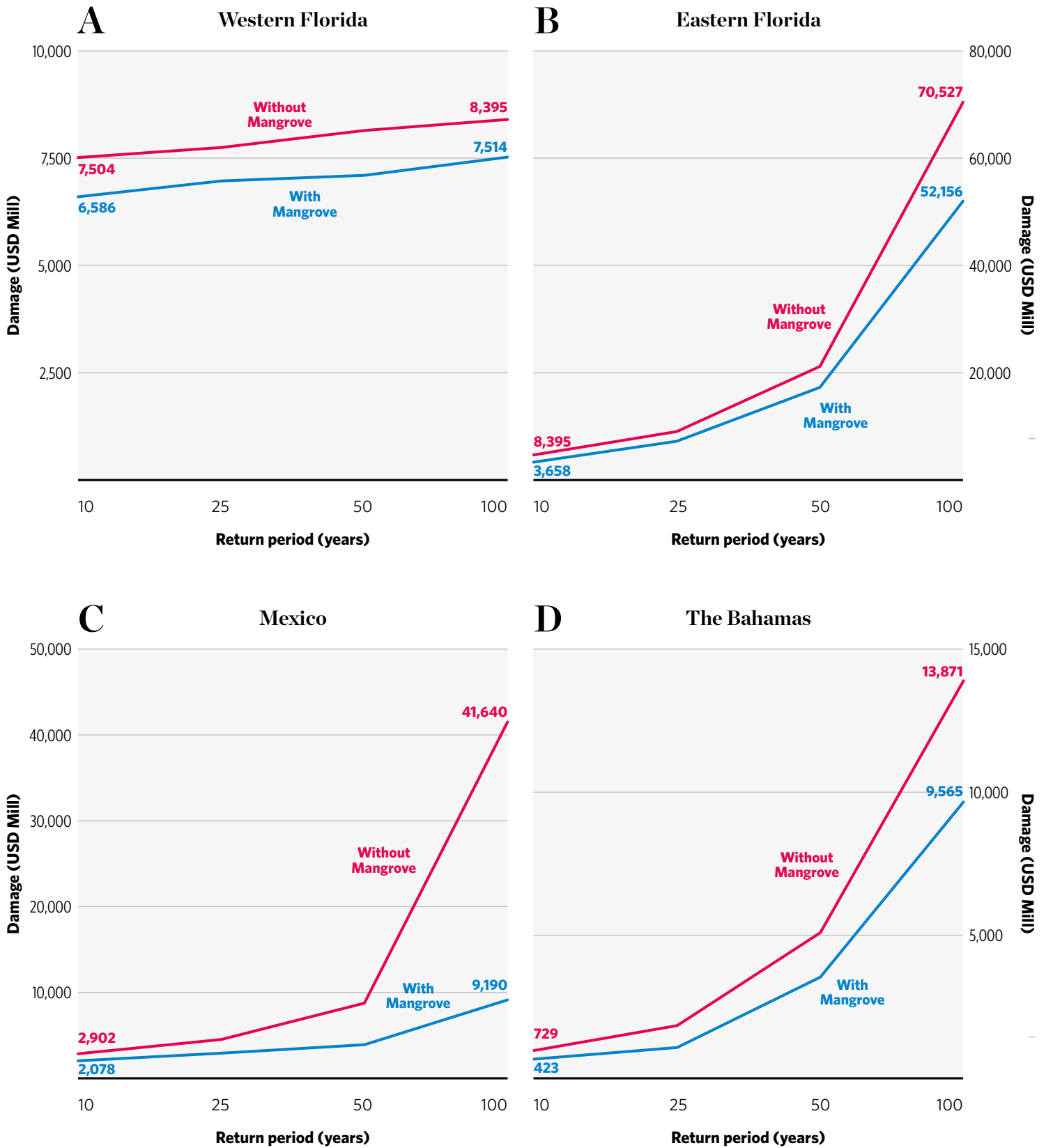


Figure 9: Flood damage with mangroves (blue line) and without mangroves (red line) per return period across (a) Western Florida, (b) Eastern Florida, (c) Mexico and (d) The Bahamas.

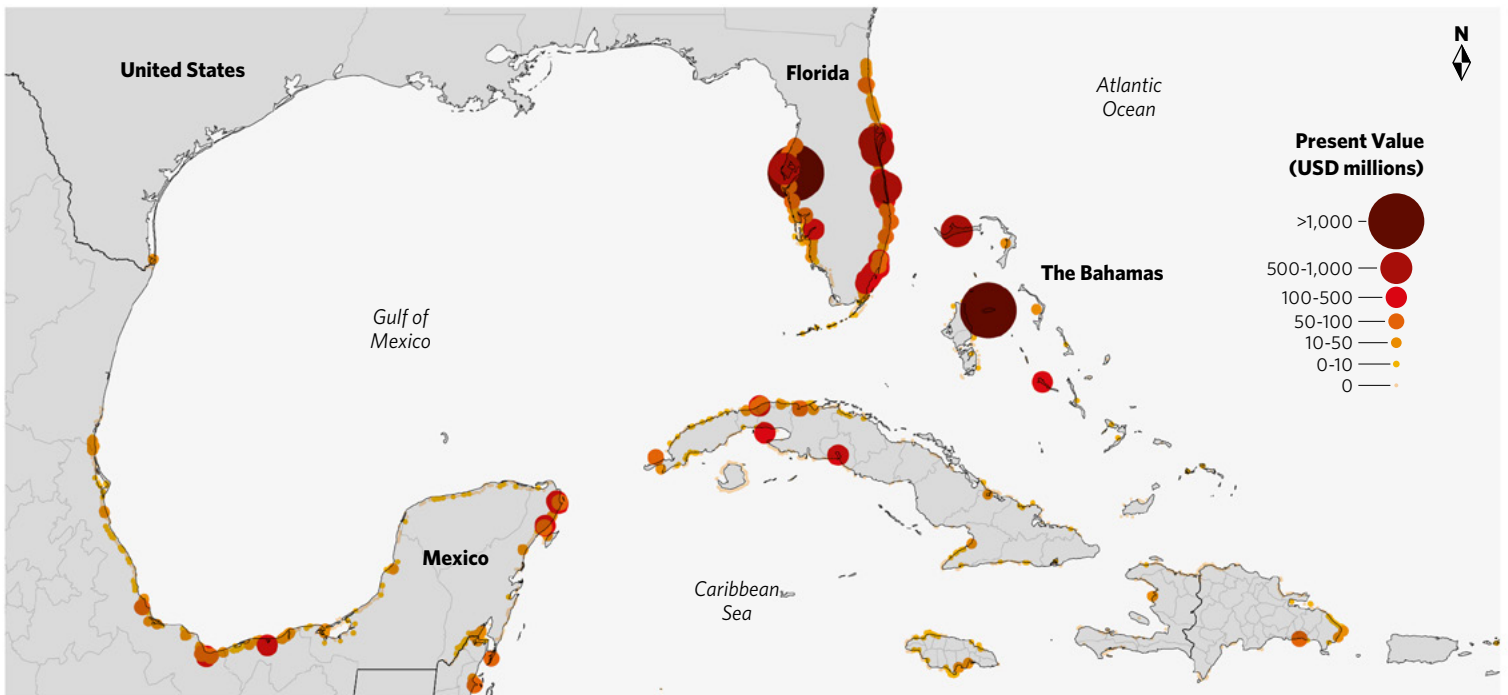


Figure 10: Present Value of mangroves at 4% discount rate for 30 years, per 5 km coastline.

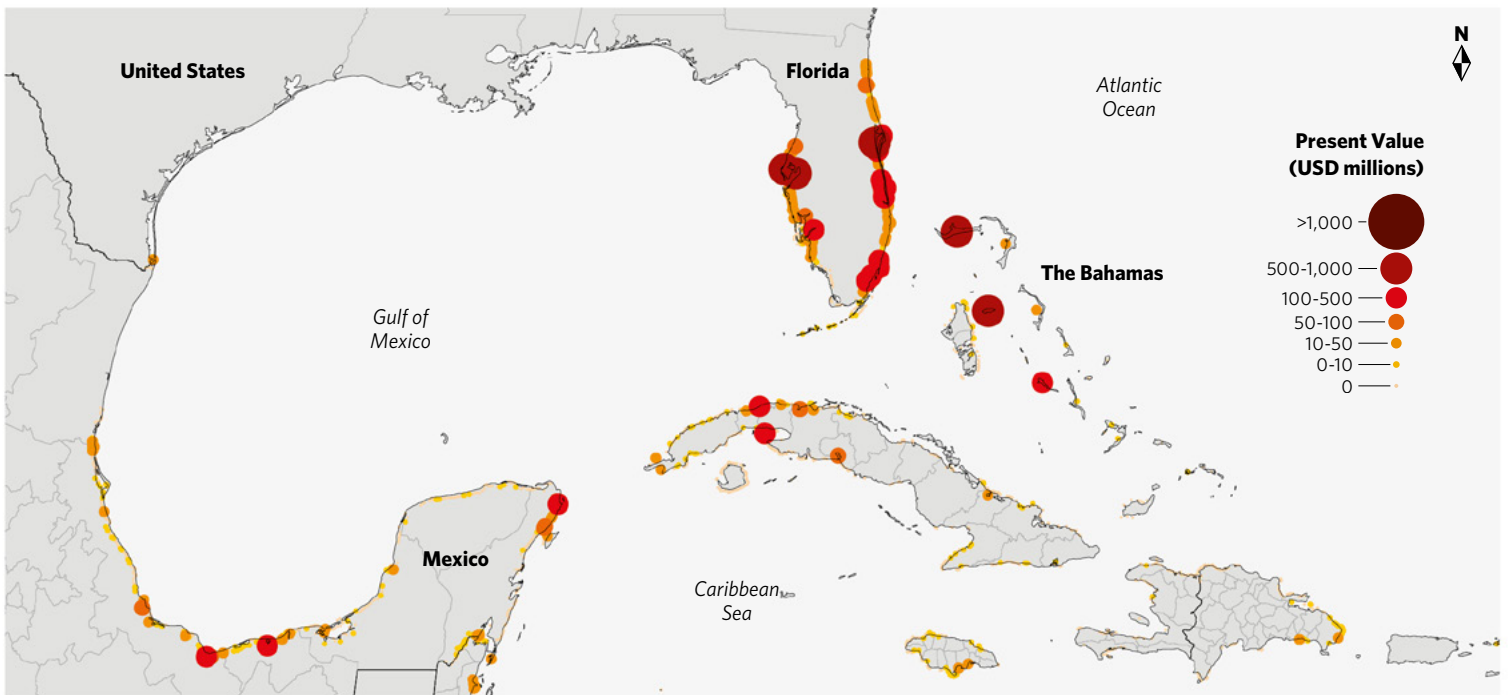


Figure 11: Present Value of mangroves at 7% discount rate for 30 years, per 5 km coastline.

At a discount rate of 7%, the mean 30-year Present Value per hectare of mangroves across the wider Caribbean in 5-km study units was \$5,877 per hectare (Figure 11 and Table 2). Among the three focal areas, The Bahamas presents the highest mean Present Value per hectare (\$39,625), followed by Florida (\$25,183), and Mexico (\$4,835). The total Present Value of mangroves across the Caribbean is \$18.28 billion. The top five regions are Florida (\$9.50 billion), Mexico (\$4.55

billion), The Bahamas (\$1.66 billion), Cuba (\$0.90 billion), and Guatemala (\$0.31 billion).

We identified eight 5-km study units where the Present Value of mangroves exceeds \$500 million (using 4% discount rate). These included six study units in Florida, around Tampa, Port St. Lucie, and just north of Palm Bay and two islands in The Bahamas.

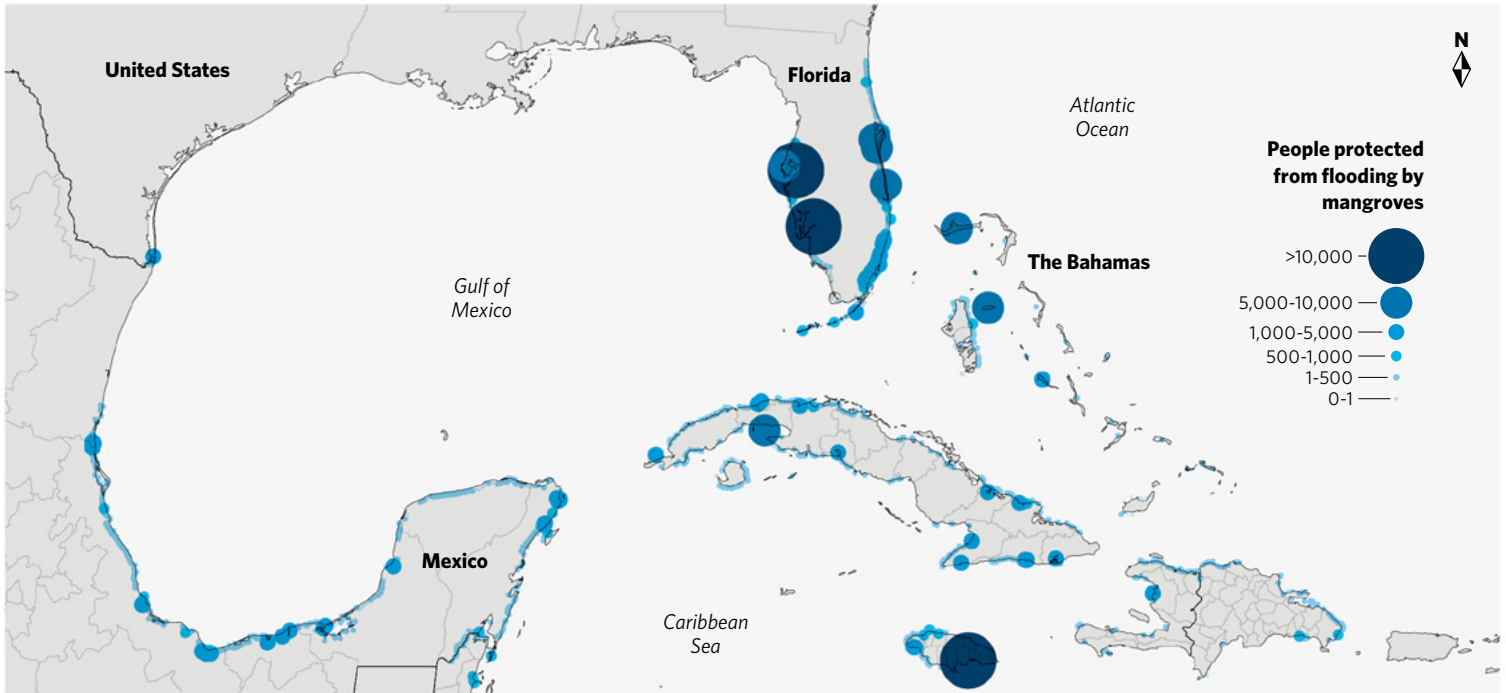


Figure 12: Annual Expected Benefits to people.

4.1.3. Annual Expected Benefits to people

We also assessed the social impact of coastal flooding and the benefits mangroves provide by protecting people (Figure 12 and Table 2). The greatest Annual Expected Benefits to people are observed in Florida, where 191,820 people receive direct flood protection from mangroves every year; followed by Mexico (110,243 people), Jamaica (49,198 people), Cuba (44,857 people), Venezuela (25,219 people) and Colombia (24,868 people). The total number of people protected from flooding by mangroves across the Caribbean is 533,187. We identified five 5-km study units in Cape Coral and Tampa (Florida), Venezuela, Jamaica and Colombia, where more than 10,000 people are protected from flooding by mangroves (Figure 12).

for 30 years, the average BCR of mangroves across the wider Caribbean in 5-km study units was 0.22 (Figure 14 and Table 2).

We analyzed the BCRs in Mexico, Florida, and The Bahamas using the median restoration cost per hectare for each country. In these three regions, we identified a significant number of opportunities for cost effective restoration. Among these areas, The Bahamas had the highest average BCR (1.52 at a 4% discount rate and 1.10 at a 7% discount rate), followed by Mexico (1.47 at a 4% discount rate and 1.07 at a 7% discount rate), and Florida (0.36 at a 4% discount rate, and 0.26 at a 7% discount rate).

4.1.4. Benefit: Cost analysis

The average BCR of mangroves across the Caribbean in 5-km study units was 0.3 at a discount rate of 4% for 30 years (Figure 13 and Table 2). At a discount rate of 7%

Some of the locations with the highest BCRs (>5) include Tampico, Campeche, Cancun, Puerto Morelos, Playa del Carmen, and Chetumal in Mexico; Fort Pierce, Jupiter, Miami, Homestead, Englewood, Osprey, and Palm Harbor in Florida; and Nassau, Grand Bahama, and Andros Town in The Bahamas.

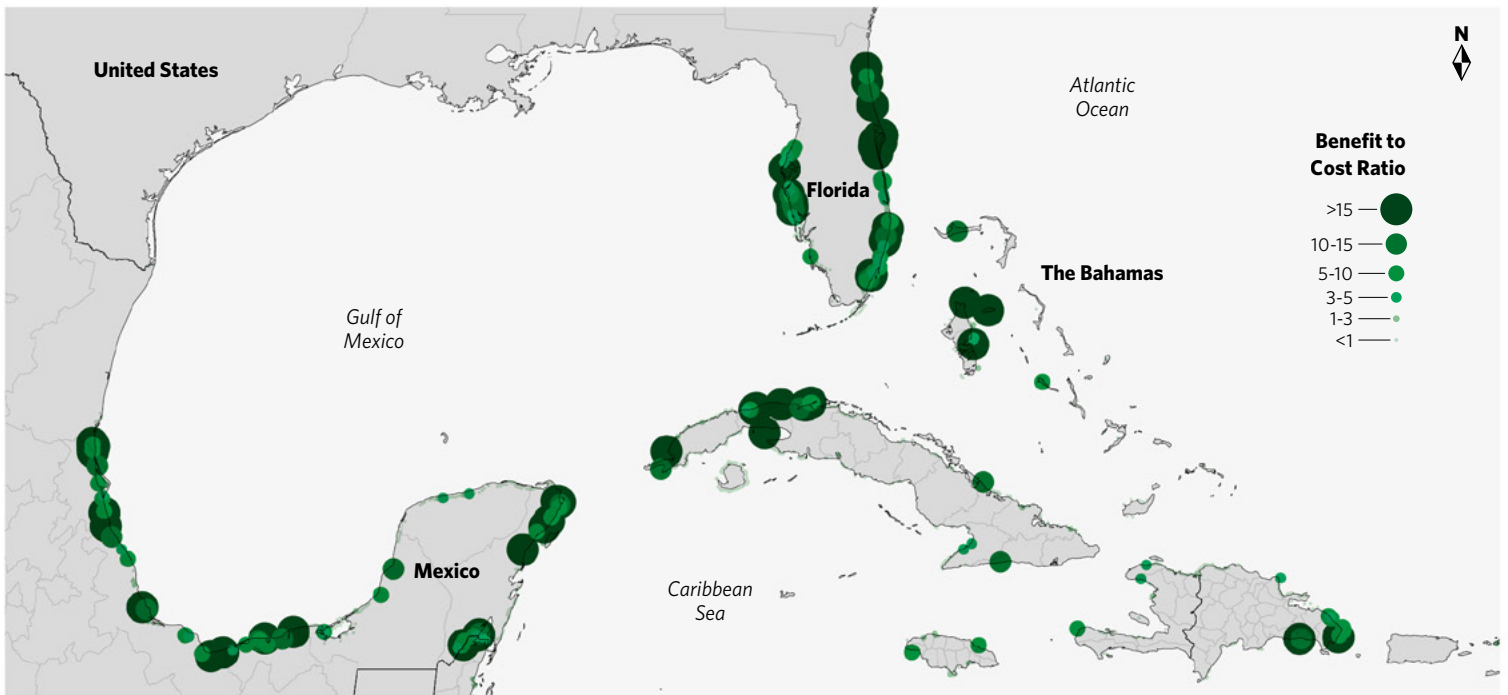


Figure 13: BCRs of mangroves at a 4% discount rate for 30 years. Values are the ratio between the Present Value (PV) of restored mangroves as an infrastructure asset assuming a 30-year project with a 4% discount rate, and the restoration costs. Benefit values are based on Menendez et al. (2020). We assume a median restoration cost of \$4,538 per hectare in Mexico, \$54,653 per hectare in western Florida, \$118,524 per hectare for projects in eastern Florida, and \$35,955 per hectare across The Bahamas. Everywhere else we assume a value of \$23,000 per hectare. The BCRs are summarized in 5 km coastal study units (see methods).

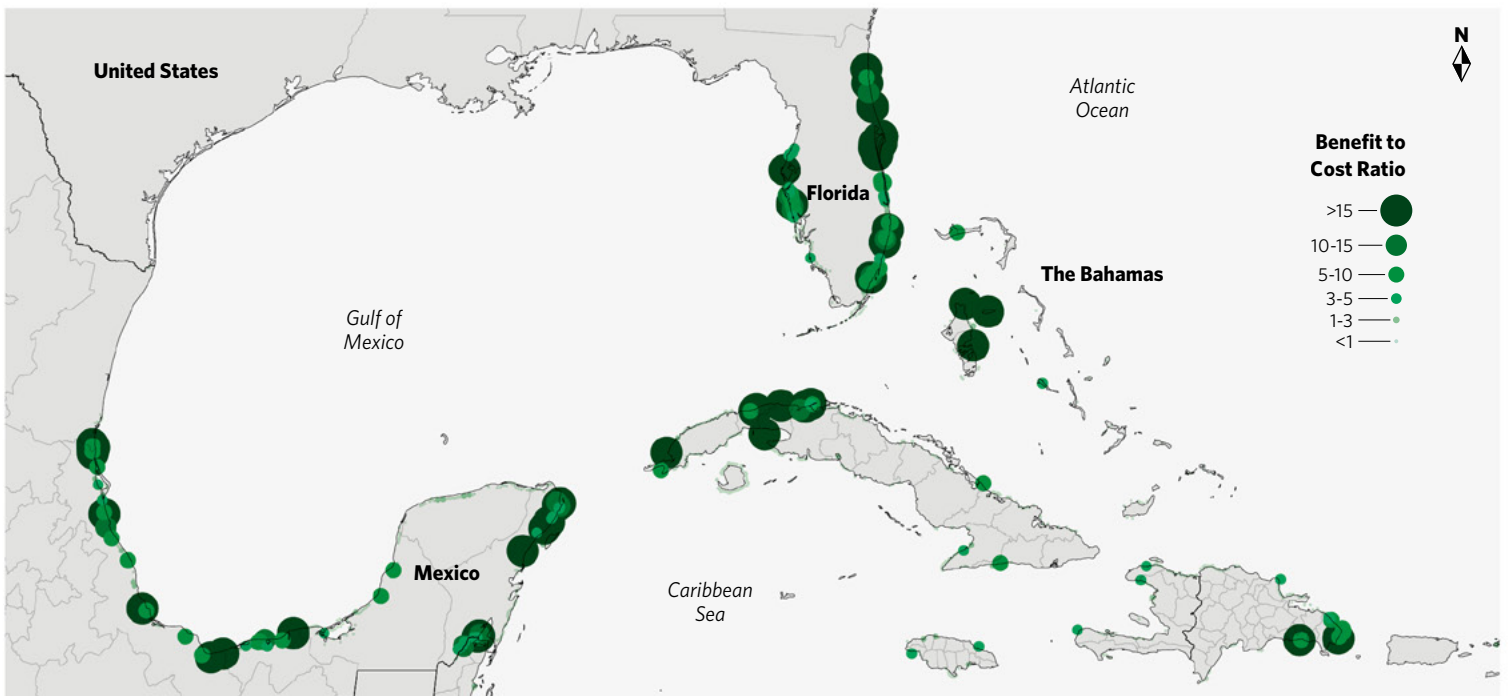


Figure 14: BCRs of mangroves at a 7% discount rate for 30 years. Values are the ratio between the Present Value (PV) of restored mangroves as an infrastructure asset assuming a 30-year project with a 7% discount rate, and the restoration costs. Benefit values are based on Menendez et al. (2020). We assume a restoration cost of \$4,538 per hectare in Mexico, \$54,653 per hectare in Western Florida, \$118,532 per hectare for projects in Eastern Florida, and \$39,599 per hectare across The Bahamas. Everywhere else we assume a value of \$23,000 per hectare. The BCRs are summarized in 5 km coastal study units (see methods).

Country	Hectares of Mangroves	Median Mangrove Restoration Cost (USD/hectare)	4% discount rate for 30 years			7% discount rate for 30 years			Annual Expected People Protected
			Present Value (USD million)	Present Value per Hectare (USD)	Benefit to Cost Ratio	Present Value (USD million)	Present Value per Hectare (USD)	Benefit to Cost Ratio	
Anguilla	432	23,000	2.31	5,343	0.23	1.68	3,880	0.17	0
Antigua and Barbuda	773	23,000	58.11	75,175	3.27	42.20	54,587	2.37	312
Bahamas	41,908	35,955	2,286.90	54,570	1.52	1,660.61	39,625	1.10	21,027
Belize	74,480	23,000	338.04	4,539	0.20	245.46	3,296	0.14	5,044
Colombia	389,980	23,000	123.90	318	0.01	89.97	231	0.01	24,868
Costa Rica	49,457	23,000	314.97	6,369	0.28	228.71	4,624	0.20	9,810
Cuba	441,610	23,000	1,243.04	2,815	0.12	902.62	2,044	0.09	44,857
Dominica	159	23,000	0.69	4,367	0.19	0.50	3,171	0.14	0
Dominican Republic	23,685	23,000	197.77	8,350	0.36	143.61	6,063	0.26	4,156
Grenada	191	23,000	0.04	189	0.01	0.03	137	0.01	0
Guatemala	27,827	23,000	423.71	15,227	0.66	307.67	11,057	0.48	5,553
Honduras	124,590	23,000	23.72	190	0.01	17.22	138	0.01	4,828
Haiti	17,588	23,000	21.26	1,209	0.05	15.43	878	0.04	19,600
Jamaica	10,060	23,000	155.09	15,417	0.67	112.62	11,195	0.49	49,198
Saint Lucia	170	23,000	0.00	0	0.00	0.00	0	0.00	0
Mexico	940,170	4,538	6,260.61	6,659	1.47	4,546.07	4,835	1.07	110,243
Nicaragua	73,906	23,000	386.88	5,235	0.23	280.93	3,801	0.17	6,129
Panama	141,490	23,000	235.68	1,666	0.07	171.13	1,210	0.05	9,077
Turks and Caicos	3,430	23,000	3.25	948	0.04	2.36	689	0.03	701
Trinidad and Tobago	6,286	23,000	0.33	53	0.00	0.24	39	0.00	745
US (Florida)	377,100	97,580	13,077.83	34,680	0.36	9,496.32	25,183	0.26	191,820
Venezuela	364,790	23,000	18.75	51	0.00	13.61	37	0.00	25,219
US Virgin Islands	172	23,000	2.07	12,017	0.52	1.50	8,726	0.38	0
All Caribbean	3,110,082	27,109	25,172.86	8,094	0.30	18,279.00	5,877	0.22	533,187

Table 2: Summary table highlighting extent of mangrove forests, restoration costs, present value, and benefit cost ratios at 4% and 7% discount rates for a 30-year period, and people protected across 23 geographies in the wider Caribbean.

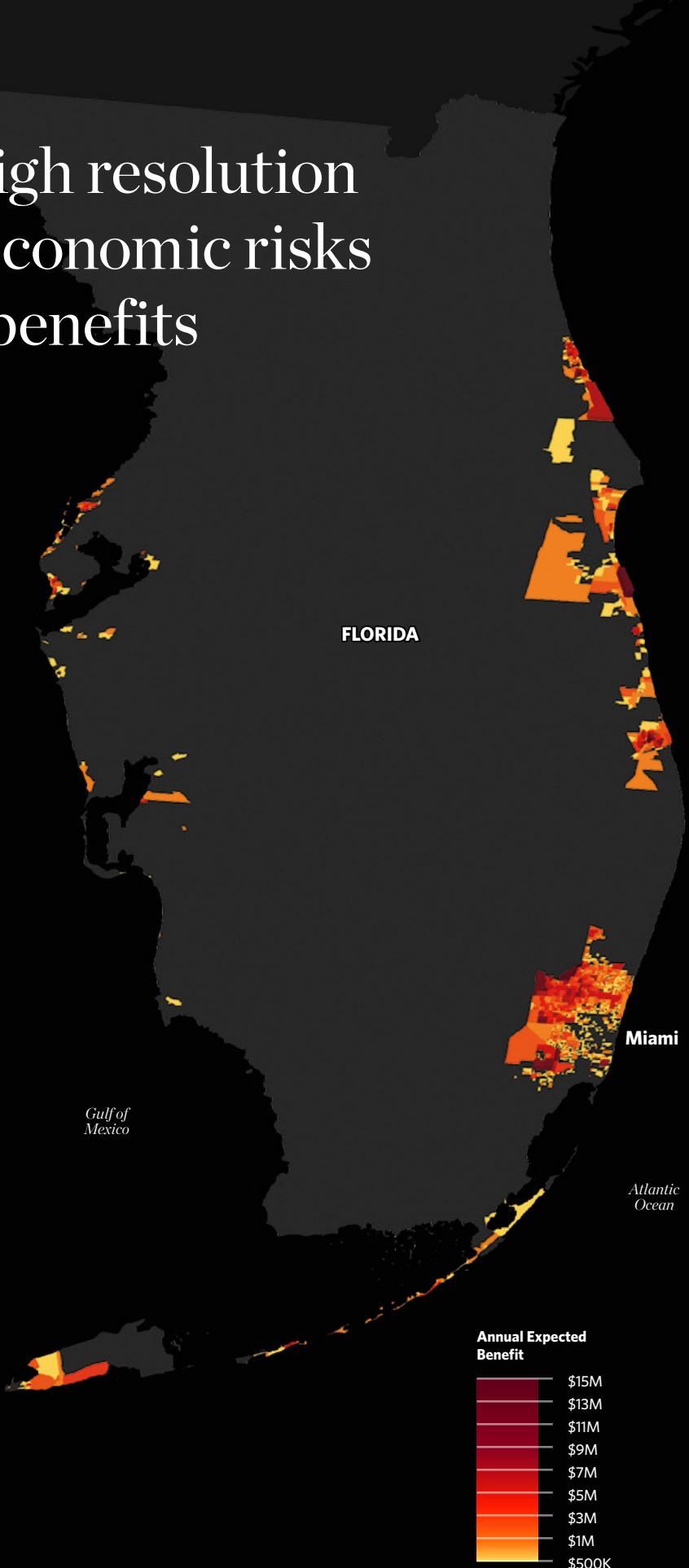
4.2. Florida: High resolution assessment of economic risks and mangrove benefits

Figure 15: Annual Expected Benefits of mangroves for flood reduction to property by Census Block Group across Florida using NSI data and USACE depth-damage curves with the FEMA FAST tool. There are some benefits around Lake Okeechobee because there was some flooding observed far inland in the most extreme event in the global flood model that was reduced by mangroves.

4.2.1. Annual Expected Benefit and Present Value of mangroves using NSI data

In Florida, we used the high-resolution NSI data and the FEMA FAST tool with the USACE structure-specific depth-damage curves to assess flood risk and mangrove benefits across the state. These high-resolution data allow us to assess variation in risk and benefit at a variety of scales relevant to decision-making. Figure 15 and Figure 16 illustrate results at the Census Block Group, but other relevant units are possible including municipalities and county.

Using NSI data and better depth-damage curves, the Annual Expected Benefit of mangroves was calculated at \$2.7 billion per year statewide. Applying discount rates of 4% and 7% for a 30-year period, NSI yields a statewide Present Value of mangrove benefits at \$50 billion and \$37 billion, respectively.



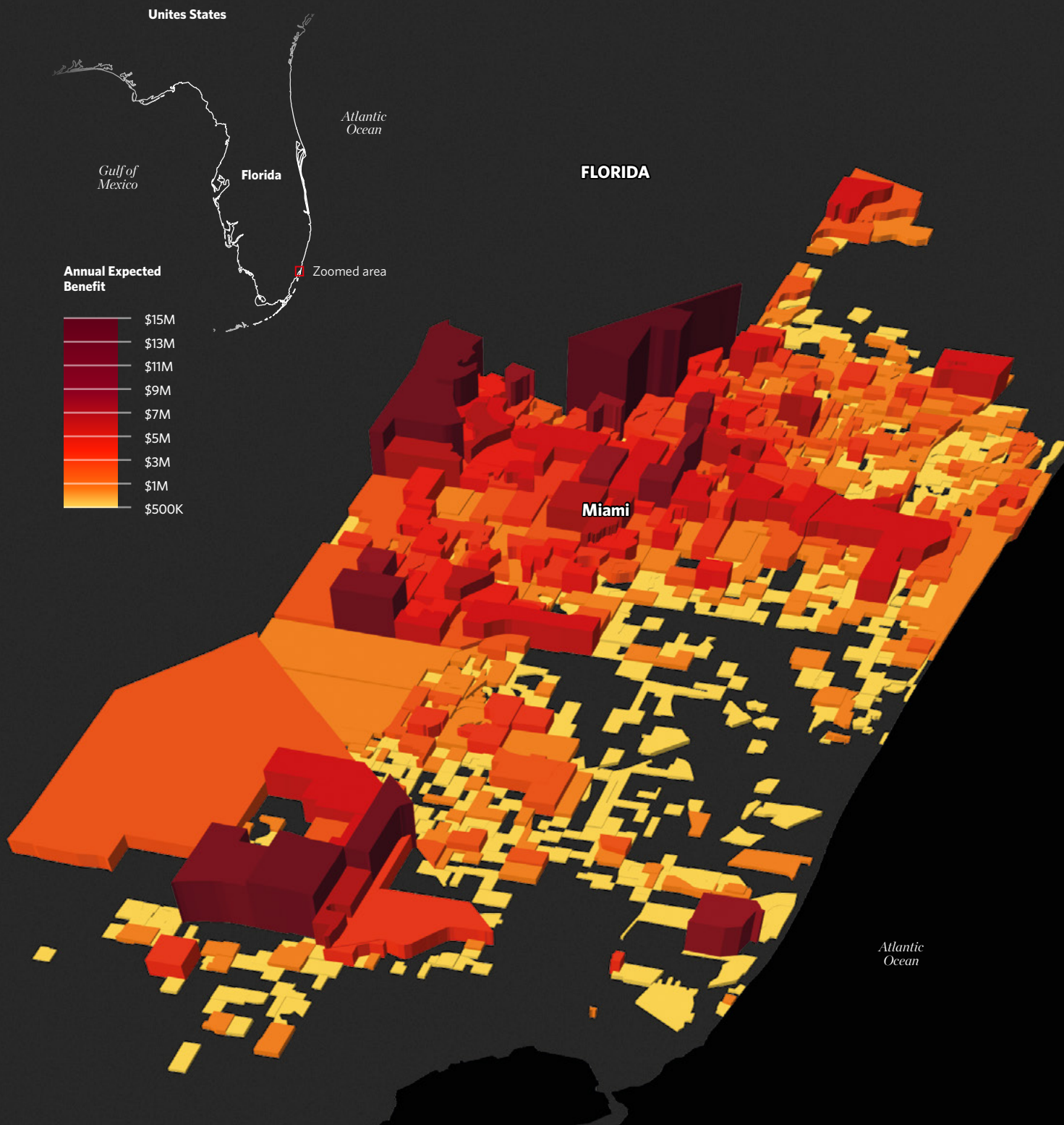
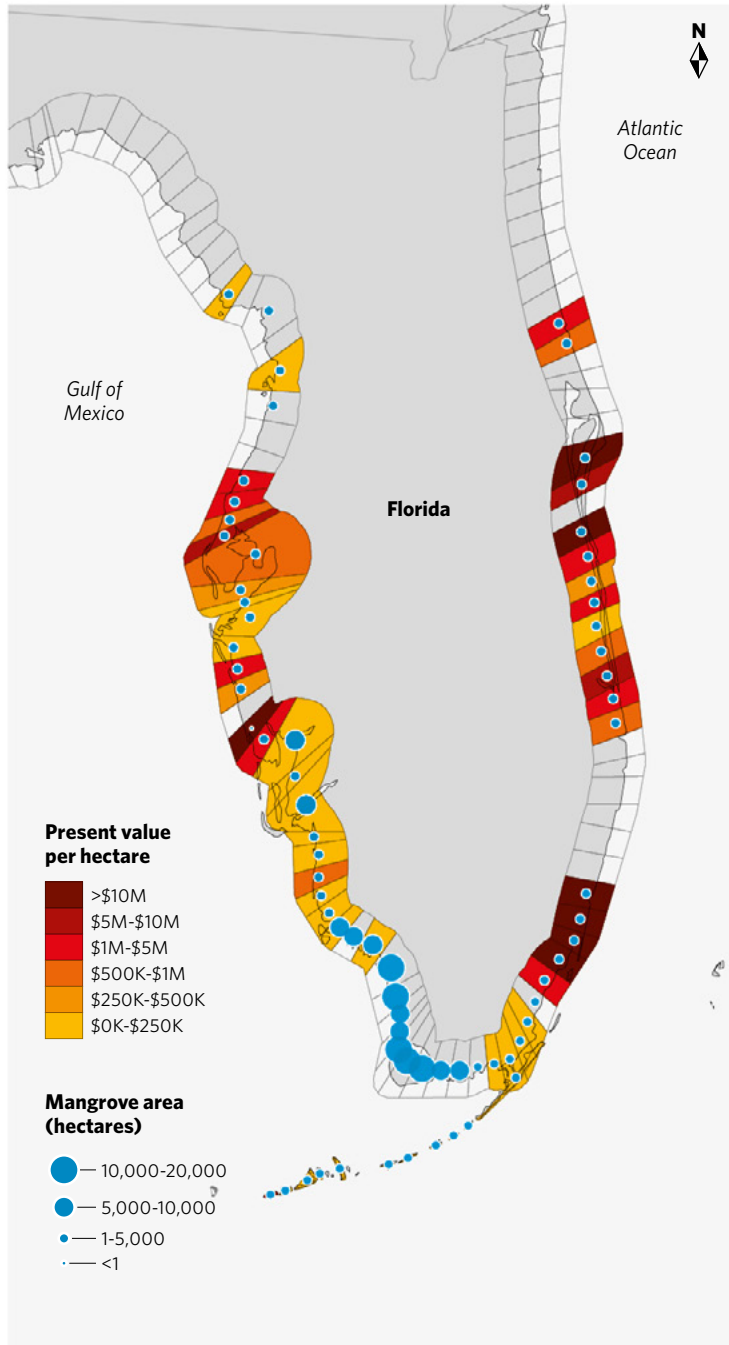


Figure 16: Annual Expected Benefits of mangroves for flood reduction to property around Miami, Florida. Results are summarized at the Census Block Group level using NSI data and USACE depth-damage curves with the FEMA FAST tool. Inland benefits arise for numerous reasons based on the distribution of mangroves, waterways, and building values and also because benefits arise from the difference in flood extents and heights; sometimes areas near the coast are flooded both with and without mangroves.

A 4% discount rate for 30 years



B 7% discount rate for 30 years

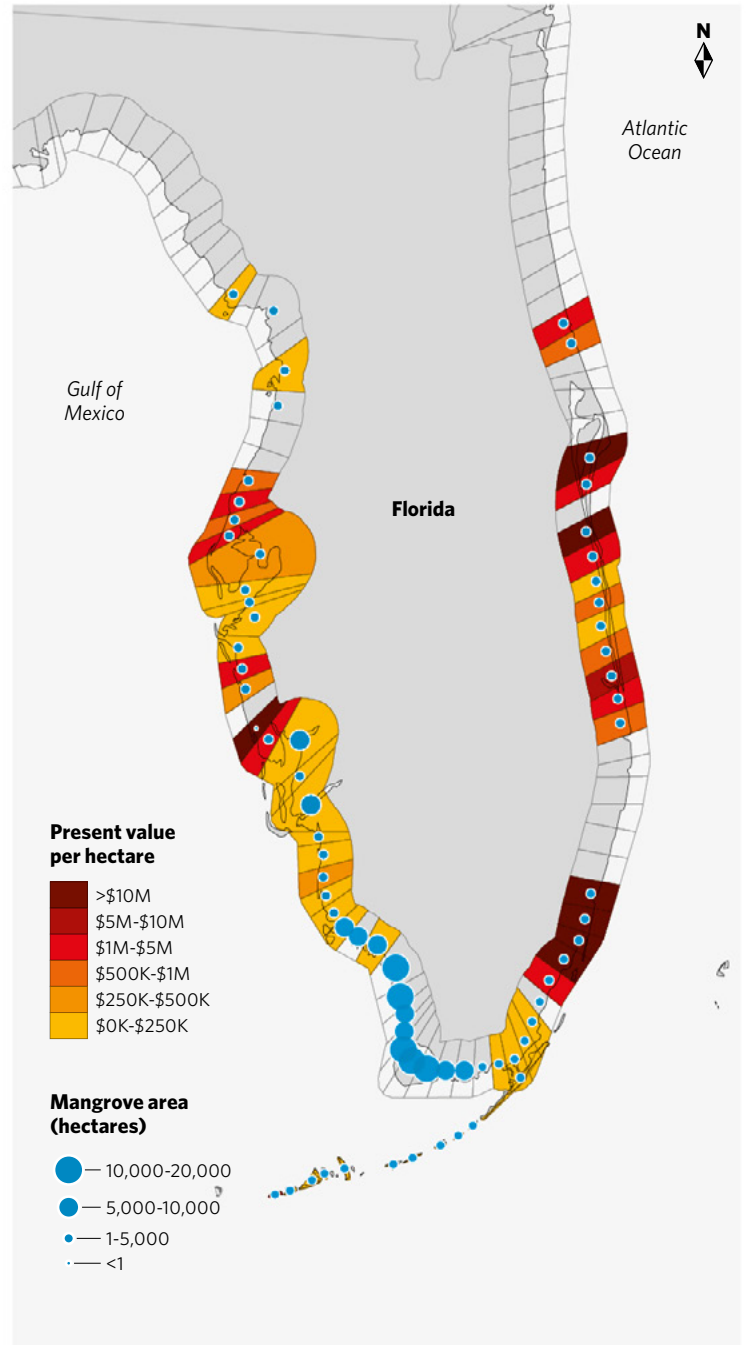
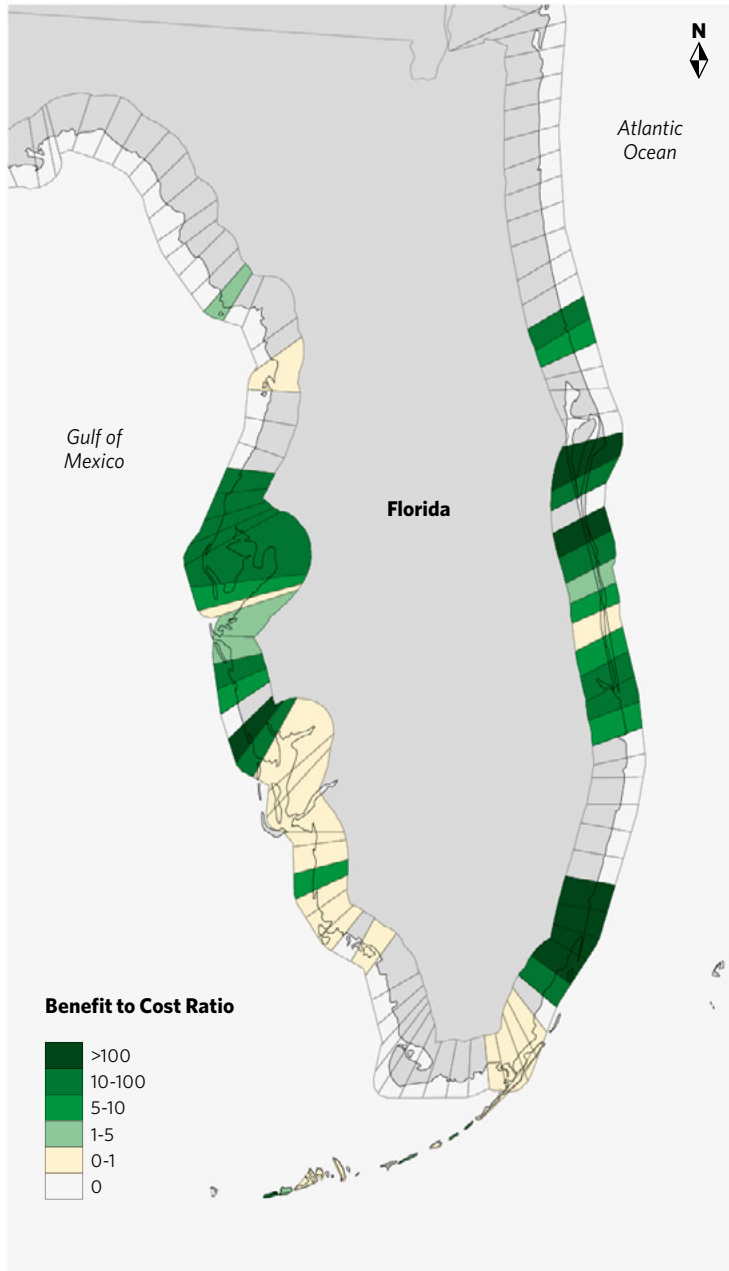


Figure 17: Present Value per hectare of mangroves for 5-km study units in Florida, based on NSI and FEMA FAST, using a 4% (panel a) and 7% (panel b) discount rate over a 30-year period. Average values per hectare are low in some areas, particularly in southwest Florida where the total asset value is low and the total abundance of mangroves is high within the study units.

We also summarized the results in the 5-km study units. We identified areas with mangroves across more than 100 kms of coastline in Florida where the Present Value of mangroves exceeds \$1 million per hectare, based on NSI data and USACE depth-damage curves using a 4% discount rate and 30-year period (Figure 17, a).

The results with a 7% discount rate and 30-year period, are similar, with 90 kms of coastline valued at over \$1 million per hectare (Figure 17, b). These highly valuable mangrove forests exist along the coast of central and southern Florida.

A 4% discount rate for 30 years



B 7% discount rate for 30 years

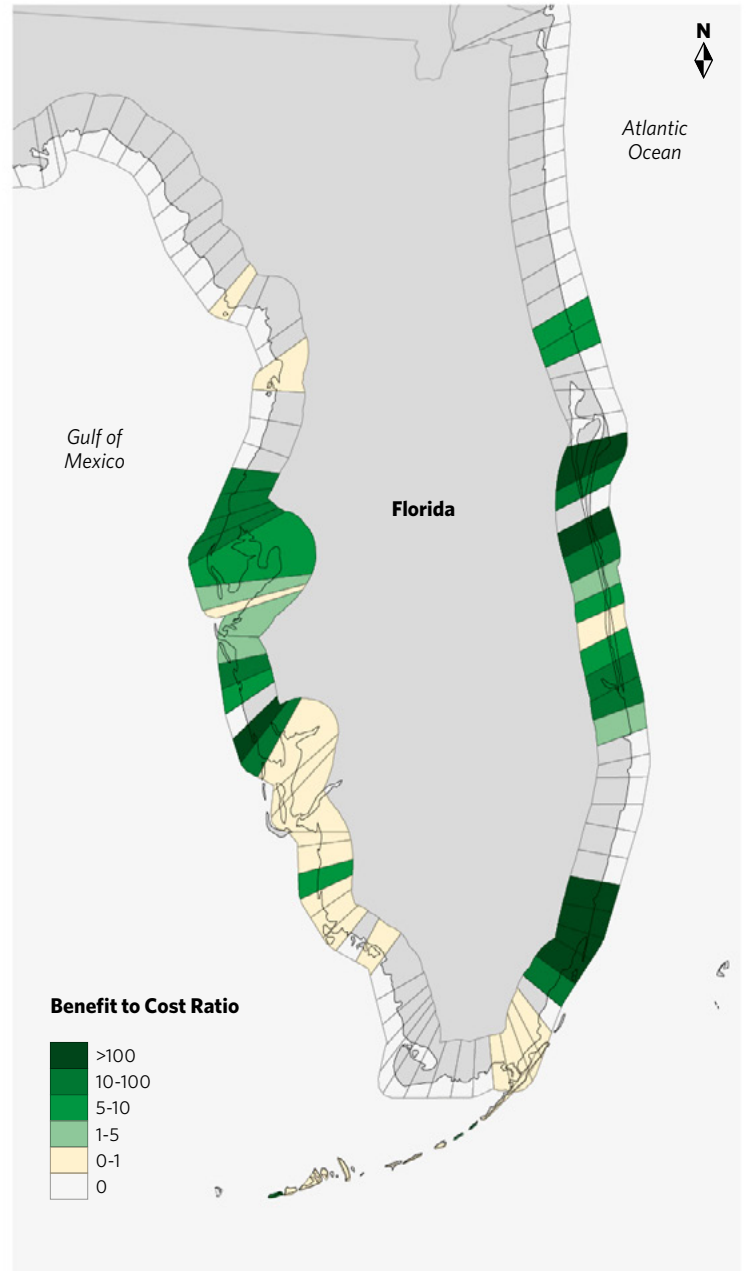


Figure 18: Benefit cost ratios (BCR) of mangrove restoration projects in Florida at 4% (left) and 7% (right) discount rates for 30 years. Results are presented in 5-km study units. BCRs are low in some areas where mangroves are very abundant and total asset value is relatively low (e.g., southwest Florida). The addition of a hectare of mangroves in these areas has only marginal value on average. However, if strategically placed in front of key assets, mangroves could have high benefits even in these areas.

4.2.2. Benefit to Cost Ratios using NSI data

We used the NSI results and the project cost data presented earlier (Table 1) to assess the BCRs for mangrove restoration in Florida, assuming a 4% discount rate and a

fixed 30-year return period. For the median cost estimate (\$54,653 per hectare in western Florida, \$118,524 per hectare in eastern Florida), this yielded 33 5-km study units distributed across southern and central Florida and the Florida Keys, where mangrove restoration is likely to be cost effective (Figure 18).

4.3. Using fragility curves to assess likelihood of mangrove loss to storms

We used the data in Han et al. (2018) to identify mangrove damage values (Figure 19, panel A and B) and developed a regression analysis to describe the fragility curve (Equation 1). We found a positive correlation between wind speed and percent of mangrove loss (Figure 19, panel C):

$$D(\%) = 0.0026 \cdot \text{Wind}(\text{knots}) - 0.1242 \text{ if } \text{Wind} > 60\text{knots} \text{ Eq., 1}$$

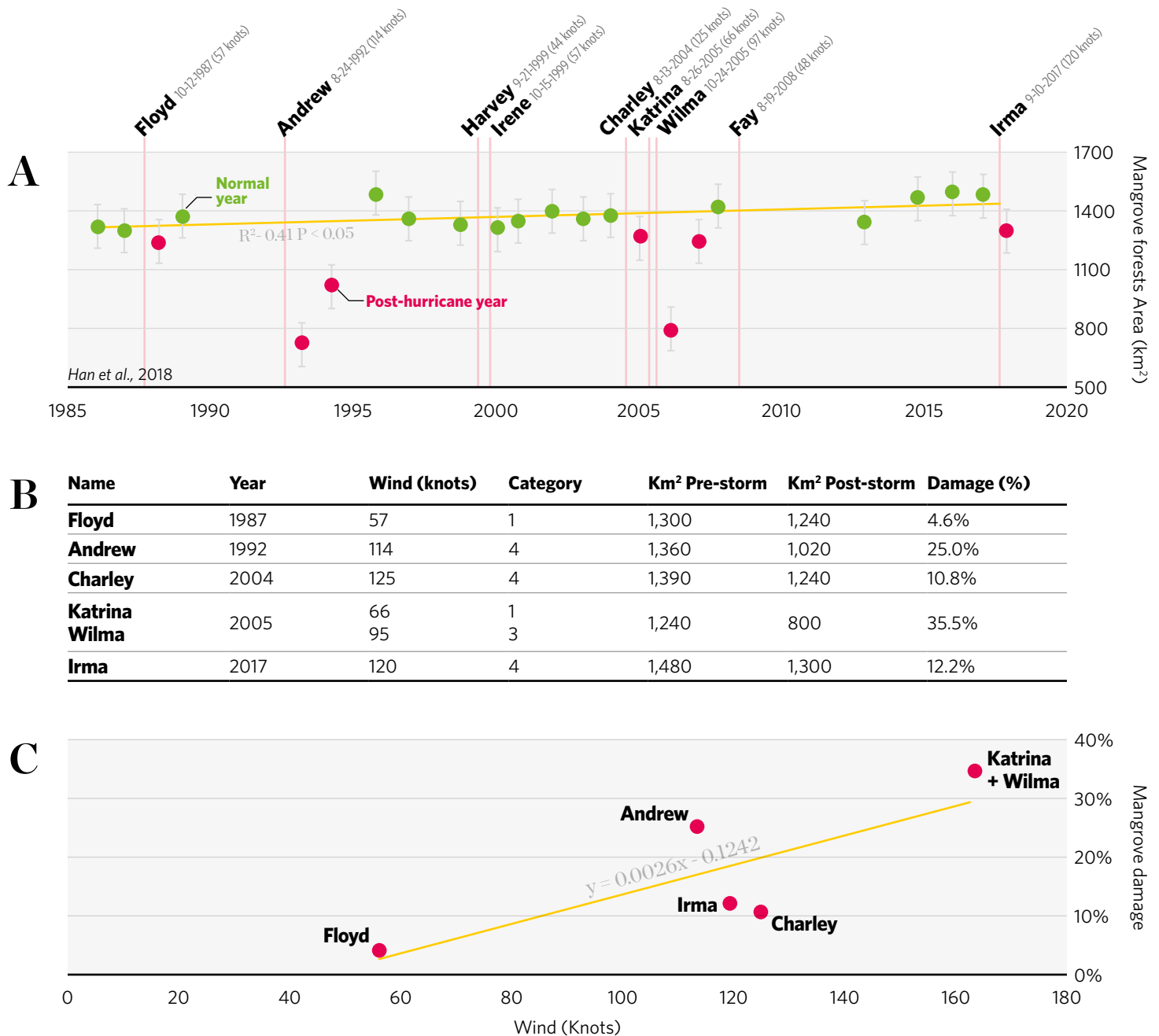


Figure 19: The mangrove fragility curve was developed using original data from Han et al. (2018) that shows changes in mangrove forest area after 9 tropical cyclones (A); values derived from (A) connecting damage and wind speed (B); and linear regression between wind speed and mangrove loss (C).

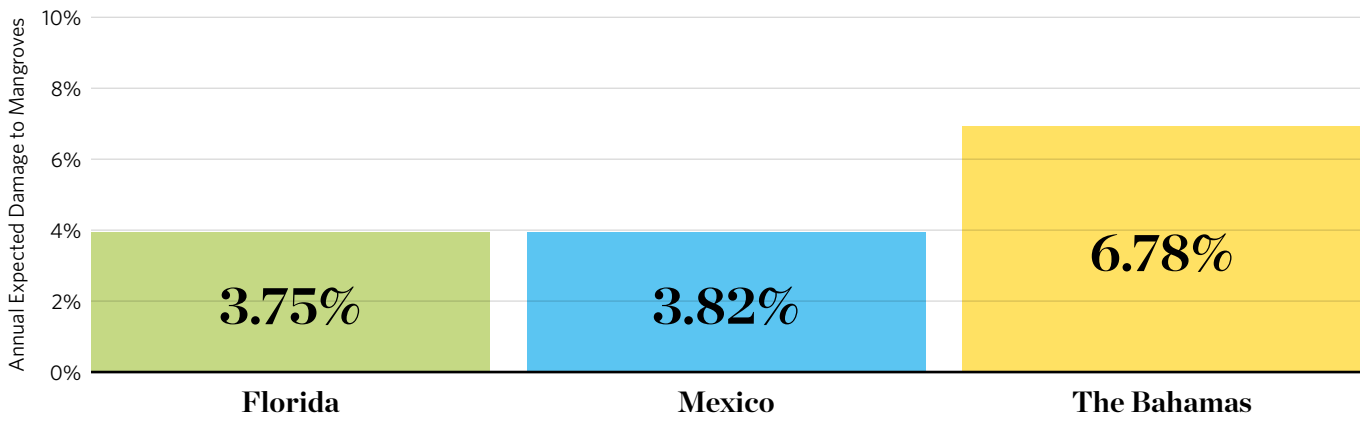


Figure 20: Annual Expected Damage of mangroves (%) produced by tropical cyclones in Florida (green), Mexico (blue), and The Bahamas (yellow).

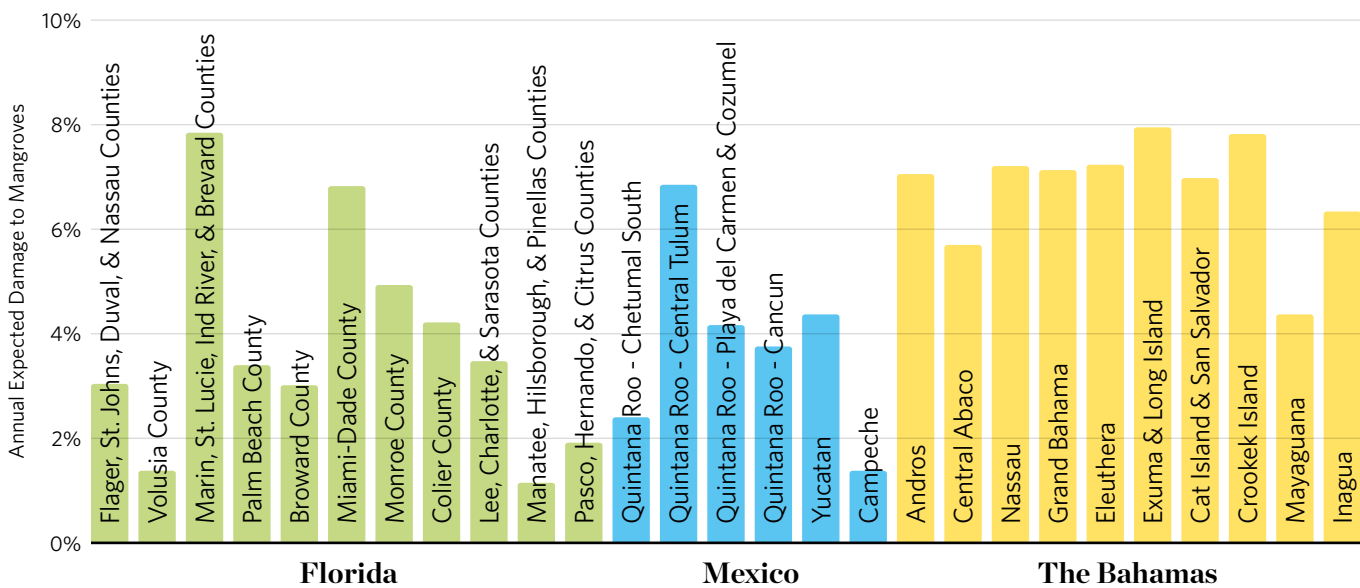


Figure 21: Annual Expected Damage of mangroves (%) produced by tropical cyclones at the regional subdivisions across Florida (green), Mexico (blue), and The Bahamas (yellow).

Based on the fragility curve expressed in Equation 1 and spatial variation in predicted storm wind speeds, we estimated the likely annual expected loss of mangroves from storms across Mexico, Florida, and The Bahamas. Predicted storm losses of mangroves varied (Figure 20), with the highest percent losses in The Bahamas (6.8%), followed by Mexico (3.8%), and Florida (3.8%).

There is substantial variability in the Annual Expected Damage to mangrove habitats across the 27 subregions in Mexico, Florida, and The Bahamas (Figure 21). In Mexico, the Central region of Quintana Roo experiences 6.85% of annual mangrove loss, while only 1.4% of

mangroves in Campeche are expected to be damaged by tropical storms. Expected losses in Florida were especially variable: study units in Martin, St. Lucie, Indian River, and Brevard counties had expected losses of mangroves of 7.9%, while study units in Manatee, Hillsborough, Pinellas, and Volusia counties had much lower predicted annual losses of mangroves of approximately 1.4%. In The Bahamas, all the islands have more than 4% of expected losses. The highest damage is expected to happen in Exuma and Long Island (7.9%), followed by Crooked Island (7.8%). The island of New Providence where the capital, Nassau, is located had 7.2% Annual Expected mangrove loss.



Sub-adult lemon sharks cruise along the edge of the mangroves in Bimini, The Bahamas. © Jillian Morris/TNC.

5. Discussion

There are many opportunities for investments in mangroves given their substantial flood protection benefits, wide distribution and relatively cheap costs of restoration. In these analyses we show that mangroves across the Caribbean and Florida have flood reduction benefits that substantially outweigh likely costs of restoration. In many areas we show that mangrove restoration can yield returns on investment of 15:1 or greater.

It is known that restoration costs can be highly variable so specific benefit to cost ratios should be taken as guides for where ROIs are likely to be high. However, the maps of Present Value (PV) do provide a strong indication of the scale of restoration benefits and where benefits are likely to well exceed any costs of restoration. Some 5-km study units have present values for mangrove flood protection benefits that exceed \$500 million over a 30-year period. Some states and countries have average present values per hectare in the hundreds of thousands of dollars. That is as long as restoration costs are less than, say, \$100,000 per hectare then benefits would well exceed costs in many areas.

With out fragility curves, we show that mangroves face significant impacts themselves from storms. Mangroves, however, can recover rapidly after storms and this could be hastened with timely investments in restoration. Elsewhere data shows that marshes and mangroves in Florida recover from hurricanes more rapidly if they are in managed areas (Castagno et al. 2021, Lagomasino et al. 2021).

Our efforts represent state-of-the-art process-based assessments of flood risk and mangrove benefits across

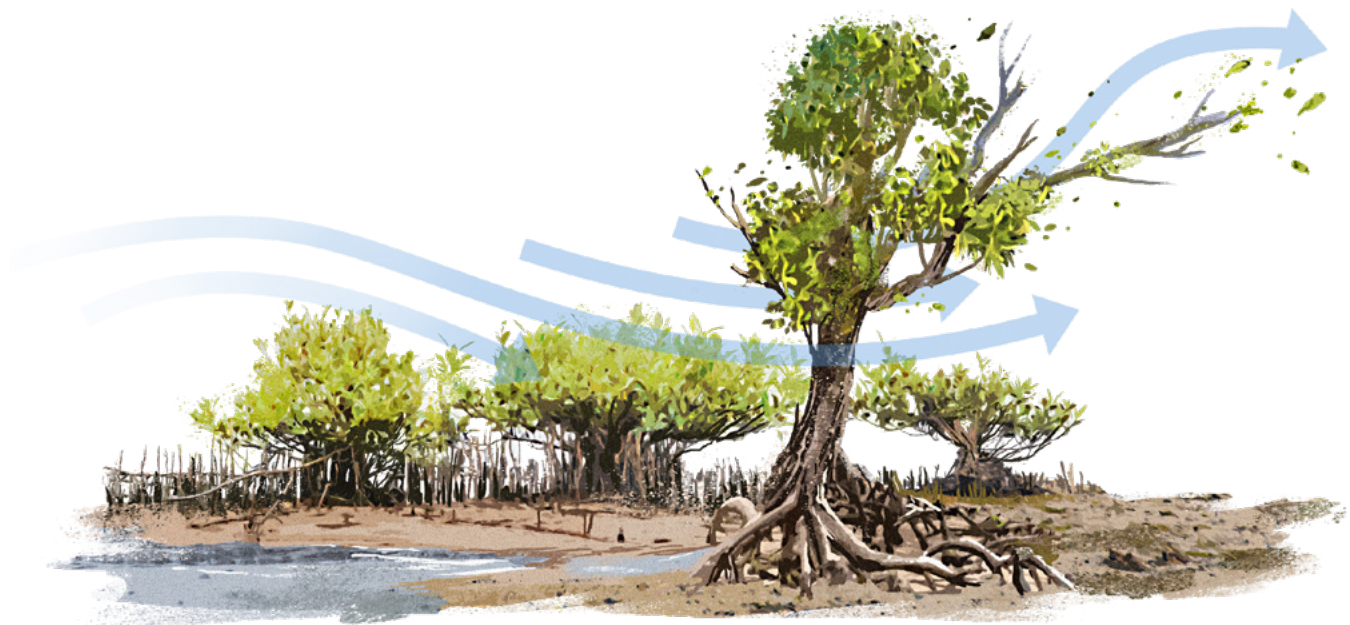
the wider Caribbean. For most countries with mangroves, these represent the best data and models for estimating mangrove benefits and, for many of these countries, the best national level estimate of flood risk. Based on prior work and our own sensitivity analyses, the greatest sources of uncertainty in coastal flood risk assessments are estimates of topography (Menéndez et al., 2019). In addition, nearshore bathymetry remains a major gap, though there are advances in remote sensing that could help improve flood risk assessments. For mangrove coverage, we have only the extent of mangroves and not information on age, density, species, degree of degradation, or other factors, which can all affect the capacity of mangroves to reduce flooding. We used mangrove distribution data from 2010 but more up to date information is becoming available, for example, through the Global Mangrove Watch project. Major remaining constraints for global coastal flooding models include the consideration of flooding as a one-dimensional process and the difficulty in representing flooding well on smaller islands.

There are limitations to these BCRs, but overall, we expect them to be conservative for several reasons. First, we do not consider indirect benefits from averted flooding, such as avoided business interruption, which are usually more than two times larger than direct benefits (Sultana et al., 2018). We also do not add values from additional ecosystem services, such as carbon sequestration (Jakovac et al., 2020), tourism (Spalding et al., 2019), and fish production (Hutchison et al., 2014). We do not factor in changes in sea level rise (Kopp et al., 2014) or storminess (Knutson et al., 2021) that are associated with climate change, which would increase flooding and in most cases the benefits from mangroves for flood reduction.

By comparing mangrove benefits from using NSI data with that from GAR data, we see very similar patterns in the Florida results overall. However, the Florida present value of mangrove benefits over 30 years with a 4% discount rate based on NSI (\$50 billion) are higher than those based on the GAR data in our global analyses (\$13.10 billion). We expect the main reason for this difference to be from the depth-damage curves (Figures 3 and 4).

These results open new opportunities to support restoration of mangroves with funds from hazard mitigation, climate adaptation, and disaster recovery. For example, in the U.S., FEMA pre-disaster mitigation grant funding was \$660 million in 2020 and post-disaster funding from FEMA and other agencies ranges from tens to hundreds of billions of dollars annually (Airoldi et al., 2021; Reguero et al., 2020). To date, very little of these funds have been used to support the restoration of habitats for risk reduction and adaptation, largely because data on benefits and costs were missing (Airoldi et al., 2021).

Some of the biggest funders of risk reduction include emergency management agencies, development banks, and reinsurers. These funders are beginning to consider how to invest in coastal habitat restoration to reduce future risk and build resilience (Airoldi et al., 2021; National Academies of Sciences and Medicine, 2019; Reguero et al., 2020). FEMA has recently reduced BCR requirements to make it easier to support nature-based projects with flood mitigation and disaster recovery funds. FEMA has indicated that BCRs could be 0.75:1 for nature-based flood reduction if an additional 0.25:1 in benefits to costs can be quantified from other services, such as carbon sequestration. In 2021, they identified \$1.16 billion in new funding opportunities, including for Building Resilient Infrastructure and Communities, which have stated priorities for nature-based solutions (FEMA, 2020). Reinsurers have sold policies to protect reefs and are developing approaches that could be used to invest in restoration up front to build resilience and reduce future payouts (Kousky & Light, 2019; Reguero et al., 2020).





Mangrove seedlings growing in mudflat at Woburn Bay MPA (Marine Protected Area), Grenada. © Marjo Aho.

6. Conclusion

We can rigorously quantify the value of mangroves for flood reduction and show that they provide significant benefits to people and property across Florida and the Caribbean. These results are clear from global data and for high resolution structure and asset data in Florida assessed with tools from FEMA and USACE. The benefits of mangroves for flood reduction alone are likely to often well exceed costs of restoration across more than 20 countries in the Caribbean. Mangroves can be damaged by storms and this fragility is also quantifiable. Timely investments in mangrove restoration after storms could hasten their recovery.



Literature cited

- Airoldi, L., Beck, M. W., Firth, L. B., Bugnot, A. B., Steinberg, P. D., & Dafforn, K. A. (2021). Emerging solutions to return nature to the urban ocean. *Annual Review of Marine Science*, 13, 445–477.
- Bayraktarov, E., Saunders, M. I., Abdullah, S., Mills, M., Beher, J., Possingham, H. P., Mumby, P. J., & Lovelock, C. E. (2016). The cost and feasibility of marine coastal restoration. *Ecological Applications*, 26(4), 1055–1074.
- Beck, M. W., Heck, N., Narayan, S., Menéndez, P., Reguero, B. G., Bitterwolf, S., ... & Losada, I. J. (2022). Return on investment for mangrove and reef flood protection. *Ecosystem Services*, 56, 101440.
- Beck, M. W., Lange, G. M., & Accounting, W. (2016). *Managing coasts with natural solutions: Guidelines for measuring and valuing the coastal protection services of mangroves and coral reefs*. The World Bank.
- Beck, M. W., Losada, I. J., Menéndez, P., Reguero, B. G., Díaz-Simal, P., & Fernández, F. (2018). The global flood protection savings provided by coral reefs. *Nature Communications*, 9(1). <https://doi.org/10.1038/s41467-018-04568-z>
- Beck, M. W., Quast, O., & Pfliegner, K. (2019). Insurance and Ecosystem-based Adaptation: Successes, Challenges and Opportunities. *Insuresilience Secretariat, Germany*.
- Bresch, D. N., & group, E. C. A. working. (2010). *Enhancing the climate risk and adaptation fact base for the Caribbean: Preliminary results of the ECA Study*. ETH Zurich.
- Bridges, T. S., King, J. K., Simm, J. D., Beck, M. W., Collins, G., Lodder, Q., & Mohan, R. K. (2021). *Overview: International Guidelines on Natural and Nature-Based Features for Flood Risk Management*.
- Burke, L., Reyntar, K., Spalding, M., & Perry, A. (2011). Reefs at risk revisited: technical notes on modeling threats to the world's coral reefs. *Washington, DC: World Resources Institute*.
- Castagno, K., Tomiczek, C. C. Shepard, M. W. Beck, A. A. Bowden, K. O'Donnell, S. B. Scyphers. 2021. Resistance, resilience, and recovery of salt marshes in the Florida Panhandle following Hurricane Michael. *Scientific Reports* 11:20381.
- Church, J. A., White, N. J., Coleman, R., Lambeck, K., & Mitrovica, J. X. (2004). Estimates of the regional distribution of sea level rise over the 1950–2000 period. *Journal of Climate*, 17(13), 2609–2625.
- Cid, A., Camus, P., Castanedo, S., Méndez, F. J., & Medina, R. (2017). Global reconstructed daily surge levels from the 20th Century Reanalysis (1871–2010). *Global and Planetary Change*, 148, 9–21.
- Compo, G. P., Whitaker, J. S., Sardeshmukh, P. D., Matsui, N., Allan, R. J., Yin, X., Gleason, B. E., Vose, R. S., Rutledge, G., & Bessemoulin, P. (2011). The twentieth century reanalysis project. *Quarterly Journal of the Royal Meteorological Society*, 137(654), 1–28.
- De Bono, A., & Chatenoux, B. (2015). A global exposure model for GAR 2015. *UNEP-GRID, GAR*.
- Desai, B., Maskrey, A., Peduzzi, P., De Bono, A., & Herold, C. (2015). *Making development sustainable: the future of disaster risk management, global assessment report on disaster risk reduction*.
- Earth Security Group (2020). *Financing the Earth's Assets: The Case for Mangroves as a Nature-based Climate Solution*
- (FEMA), F. E. M. A. (2020). *Building Community Resilience with Nature-Based Solutions: A Guide for Local Communities*. Federal Emergency Management Agency Washington, DC, USA.
- Hallegatte, S., Green, C., Nicholls, R. J., & Corfee-Morlot, J. (2013). Future flood losses in major coastal cities. *Nature Climate Change*, 3(9), 802–806.
- Han, X., Feng, L., Hu, C., & Kramer, P. (2018). Hurricane induced changes in the Everglades National Park mangrove forest: Landsat observations between 1985 and 2017. *Journal of Geophysical Research: Biogeosciences*, 123(11), 3470–3488.
- Herrera-Silveira, J. A., Teutli-Hernandez, C., Secaira-Fajardo, F., Geselbracht, L., Musgrove, M., Rogers, M., Schmidt, J., Robles-Toral, P. J., Canul-Cabrera, J. A., & Guerra-Cano, L. (2022). "Hurricane Damages to Mangrove Forests and Post-Storm Restoration Techniques and Costs." The Nature Conservancy, Arlington, VA.
- Hinkel, J., Lincke, D., Vafeidis, A. T., Perrette, M., Nicholls, R. J., Tol, R. S. J., Marzeion, B., Fettweis, X., Ionescu, C., & Levermann, A. (2014). Coastal flood damage and adaptation costs under 21st century sea-level rise. *Proceedings of the National Academy of Sciences*, 111(9), 3292–3297.
- Huizinga, J., de Moel, H., & Szewczyk, W. (2017). *Global flood depth-damage functions: Methodology and the database with guidelines*. Joint Research Centre (Seville site).
- Hutchison, J., Spalding, M., & zu Ermgassen, P. (2014). The role of mangroves in fisheries enhancement. *The Nature Conservancy and Wetlands International*, 54.
- Jakovac, C. C., Latawiec, A. E., Lacerda, E., Lucas, I. L., Korys, K. A., Iribarrem, A., ... & Strassburg, B. B. N. (2020). Costs and carbon benefits of mangrove conservation and restoration: a global analysis. *Ecological Economics*, 176, 106758.
- Kaplan, J., & DeMaria, M. (1995). A simple empirical model for predicting the decay of tropical cyclone winds after landfall. *Journal of Applied Meteorology and Climatology*, 34(11), 2499–2512.
- Knapp, K. R., Kruk, M. C., Levinson, D. H., Diamond, H. J., & Neumann, C. J. (2010). The international best track archive for climate stewardship (IBTrACS) unifying tropical cyclone data. *Bulletin of the American Meteorological Society*, 91(3), 363–376. https://doi.org/10.1007/978-90-481-3109-9_26

- Knutson, T. R., Chung, M. V., Vecchi, G., Sun, J., Hsieh, T. L., & Smith, A. (2021). Climate change is probably increasing the intensity of tropical cyclones. In *Critical issues in climate change science*. ScienceBrief Review.
- Kopp, R. E., Horton, R. M., Little, C. M., Mitrovica, J. X., Oppenheimer, M., Rasmussen, D. J., ... & Tebaldi, C. (2014). Probabilistic 21st and 22nd century sea level projections at a global network of tide gauge sites. *Earth's future*, 2(8), 383-406.
- Kousky, C., & Light, S. E. (2019). Insuring Nature. *Duke LJ*, 69, 323.
- Lagomasino, D. et. al. 2021 Storm surge and ponding explain mangrove dieback in southwest Florida following Hurricane Irma. *Nature Communications* 12:4003.
- Lange, G-M, M. W. Beck, V. Lam, P. Menéndez, R. Sumaila. 2021. Blue natural capital: mangroves and fisheries in G. M. Lange et al. (eds). *Changing Wealth of Nations 2021: Managing Assets for the Future*. World Bank.
- Losada, Í. J., Beck, M., Menendez, P., Espejo, A., Torres, S., Diaz-Simal, P., Fernandez, F., Abad, S., Ripoll, N., & Garcia, J. (2017). *Valuing protective services of mangroves in the Philippines*.
- Menéndez, P., Losada, I. J., Beck, M. W., Torres-Ortega, S., Espejo, A., Narayan, S., Díaz-Simal, P., & Lange, G.-M. (2018). Valuing the protection services of mangroves at national scale: The Philippines. *Ecosystem Services*, 34. <https://doi.org/10.1016/j.ecoser.2018.09.005>
- Menéndez, Pelayo, Losada, I. J., Torres-Ortega, S., Narayan, S., & Beck, M. W. (2020). The Global Flood Protection Benefits of Mangroves. *Scientific Reports*, 10(1). <https://doi.org/10.1038/s41598-020-61136-6>
- Menéndez, Pelayo, Losada, I. J., Torres-Ortega, S., Toimil, A., & Beck, M. W. (2019). Assessing the effects of using high-quality data and high-resolution models in valuing flood protection services of mangroves. *PLoS One*, 14(8), e0220941.
- Narayan, S., Beck, M. W., Reguero, B. G., Losada, I. J., Van Wesenbeeck, B., Pontee, N., Sanchirico, J. N., Ingram, J. C., Lange, G.-M., & Burks-Copes, K. A. (2016). The effectiveness, costs and coastal protection benefits of natural and nature-based defences. *PLoS One*, 11(5), e0154735.
- Narayan, S., Thomas, C., Matthewman, J., Shepard, C. C., Geselbracht, L., Nzerem, K., & Beck, M. W. (2019). Valuing the Flood Risk Reduction Benefits of Florida's Mangroves. *Conservation Gateway*.
- National Academies of Sciences and Medicine, E. (2019). *Building and measuring community resilience: Actions for communities and the Gulf research program*.
- Nederhoff, K., Hoek, J., Leijnse, T., van Ormondt, M., Caires, S., & Giardino, A. (2021). Simulating synthetic tropical cyclone tracks for statistically reliable wind and pressure estimations. *Natural Hazards and Earth System Sciences*, 21(3), 861-878.
- Nunes, V., & Pawlak, G. (2008). Observations of bed roughness of a coral reef. *Journal of Coastal Research*, 24 (10024), 39-50.
- Ortega, S. T., Losada, I. J., Espejo, A., Abad, S., Narayan, S., & Beck, M. W. (2019). *The Flood Protection Benefits and Restoration Costs for Mangroves in Jamaica*.
- Perez, J., Menendez, M., & Losada, I. J. (2017). GOW2 : A global wave hindcast for coastal applications. *Coastal Engineering*, 124(April), 1-11. <https://doi.org/10.1016/j.coastaleng.2017.03.005>
- Pörtner, H.-O., Roberts, D. C., Masson-Delmotte, V., Zhai, P., Tignor, M., Poloczanska, E., & Weyer, N. M. (2019). *The ocean and cryosphere in a changing climate*. Geneva: Intergovernmental Panel on Climate Change.
- Ray, R. D. (1999). *A global ocean tide model from TOPEX/POSEIDON altimetry: GOT99. 2*. National Aeronautics and Space Administration, Goddard Space Flight Center.
- Reguero, B G, Menéndez, M., Méndez, F. J., Mínguez, R., & Losada, I. J. (2012). A Global Ocean Wave (GOW) calibrated reanalysis from 1948 onwards. *Coastal Engineering*, 65, 38-55. <https://doi.org/10.1016/j.coastaleng.2012.03.003>
- Reguero, Borja G, Beck, M. W., Bresch, D. N., Calil, J., & Meliane, I. (2018). Comparing the cost effectiveness of nature-based and coastal adaptation: A case study from the Gulf Coast of the United States. *PLoS One*, 13(4), e0192132.
- Reguero, Borja G, Beck, M. W., Schmid, D., Stadtmüller, D., Raepfle, J., Schüssele, S., & Pflieger, K. (2020). Financing coastal resilience by combining nature-based risk reduction with insurance. *Ecological Economics*, 169, 106487.
- Robinson, W. D., Schmidt, G. M., McClain, C. R., & Werdell, P. J. (2000). Changes made in the operational SeaWiFS processing. *SeaWiFS Postlaunch Calibration and Validation Analyses, Part 2*, 12-28.
- Saha, S., Moorthi, S., Pan, H.-L., Wu, X., Wang, J., Nadiga, S., Tripp, P., Kistler, R., Woollen, J., & Behringer, D. (2010). The NCEP climate forecast system reanalysis. *Bulletin of the American Meteorological Society*, 91(8), 1015-1058.
- Secaira Fajardo, F., Baughman McLeod, K., & Tassoulas, B. (2019). A Guide on How to Insure a Natural Asset. *The Nature Conservancy*.
- Sheppard, C., Dixon, D. J., Gourlay, M., Sheppard, A., & Payet, R. (2005). Coral mortality increases wave energy reaching shores protected by reef flats: examples from the Seychelles. *Estuarine, Coastal and Shelf Science*, 64(2-3), 223-234.
- Spalding, M. (2010). *World atlas of mangroves*. Routledge.
- Spalding, M., & Parrett, C. L. (2019). Global patterns in mangrove recreation and tourism. *Marine Policy*, 110, 103540.
- Sultana, Z., Sieg, T., Kellermann, P., Müller, M., & Kreibich, H. (2018). Assessment of business interruption of flood-affected companies using random forests. *Water*, 10(8), 1049.
- Taille, P. J., Roman-Cuesta, R., Lagomasino, D., Cifuentes-Jara, M., Fatoyinbo, T., Ott, L. E., & Poulter, B. (2020). Widespread mangrove damage resulting from the 2017 Atlantic mega hurricane season. *Environmental Research Letters*, 15(6), 64010.
- Tatem, A. J. (2017). WorldPop, open data for spatial demography. *Scientific Data*, 4(1), 1-4.
- Tolman, H. L. (2014). WAVEWATCH III Development Group. *User Manual and System Documentation of WAVEWATCH III Version, 4*.

Building Mangrove Capital

Assessing the Benefit-Cost Ratio for Mangrove
Restoration Across the Wider Caribbean

